Lappeenranta
University of Technology

Kari Vahteristo

KINETIC MODELING OF MECHANISMS OF INDUSTRIALLY IMPORTANT ORGANIC REACTIONS IN GAS AND LIQUID PHASE

Thesis for the degree of Doctor of Science (Technology) to be presented with due permission for public examination and criticism in the Auditorium 1383 at Lappeenranta University of Technology, Lappeenranta, Finland on the 26th November 2010, at noon.

Acta Universitatis
Lappeenrantaensis 402

Supervisors Docent Jaakko Partanen
Department of Chemical Technology
Lappeenranta University of Technology
Finland

Professor Heli Sirén
Department of Chemical Technology
Lappeenranta University of Technology
Finland

Reviewers Professor Andres Öpik
Department of Basic and Applied Chemistry
Tallinn University of Technology
Viro

Professor Marita Veringa-Niemelä
Faculty of Chemistry and Materials Sciences, Chemical Technology
Aalto University
Finland

Opponent Professor Andres Öpik
Department of Basic and Applied Chemistry
Tallinn University of Technology
Viro

ISBN 978-952-214-985-5

ISBN 978-952-214-986-2 (PDF)

ISSN 1456-4491

Lappeenrannan teknillinen yliopisto

Digipaino 2010

ABSTRACT

Vahteristo Kari
Kinetic modeling of mechanisms of industrially important organic reactions in gas and liquid phase
Lappeenranta 2010
56 p.
Acta Universitatis Lappeenrantaensis 402
Diss. Lappeenranta University of Technology

ISBN 978-952-214-985-5, ISBN 978-952-214-986-2 (PDF), ISSN 1456-4491

This dissertation is based on 5 articles which deal with reaction mechanisms of the following selected industrially important organic reactions:
1. dehydrocyclization of *n*-butylbenzene to produce naphthalene
2. dehydrocyclization of 1-(*p*-tolyl)-2-methylbutane (MB) to produce 2,6-dimethylnaphthalene
3. esterification of neopentyl glycol (NPG) with different carboxylic acids to produce monoesters
4. skeletal isomerization of 1-pentene to produce 2-methyl-1-butene and 2-methyl-2-butene

The results of initial- and integral-rate experiments of *n*-butylbenzene dehydrocyclization over selfmade chromia/alumina catalyst were applied when investigating reaction 2. Reaction 2 was performed using commercial chromia/alumina of different acidity, platina on silica and vanadium/calcium/alumina as catalysts. On all catalysts used for the dehydrocyclization, major reactions were fragmentation of MB and 1-(*p*-tolyl)-2-methylbutenes (MBes), dehydrogenation of MB, double bond transfer, hydrogenation and 1,6-cyclization of MBes. Minor reactions were 1,5-cyclization of MBes and methyl group fragmentation of 1,6-cyclization products.

Esterification reactions of NPG were performed using three different carboxylic acids: propionic, isobutyric and 2-ethylhexanoic acid. Commercial heterogeneous gellular (Dowex 50WX2), macroreticular (Amberlyst 15) type resins and homogeneous *para*-toluene sulfonic acid were used as catalysts. At first NPG reacted with carboxylic acids to form corresponding monoester and water. Then monoester esterified with carboxylic acid to form corresponding diester. In disproportionation reaction two monoester molecules formed NPG and

corresponding diester. All these three reactions can attain equilibrium. Concerning esterification, water was removed from the reactor in order to prevent backward reaction.

Skeletal isomerization experiments of 1-pentene were performed over HZSM-22 catalyst. Isomerization reactions of three different kind were detected: double bond, *cis*-*trans* and skeletal isomerization. Minor side reaction were dimerization and fragmentation. Monomolecular and bimolecular reaction mechanisms for skeletal isomerization explained experimental results almost equally well.

Pseudohomogeneous kinetic parameters of reactions 1 and 2 were estimated by usual least squares fitting. Concerning reactions 3 and 4 kinetic parameters were estimated by the least-squares method, but also the possible cross-correlation and identifiability of parameters were determined using Markov chain Monte Carlo (MCMC) method. Finally using MCMC method, the estimation of model parameters and predictions were performed according to the Bayesian paradigm. According to the fitting results suggested reaction mechanisms explained experimental results rather well. When the possible cross-correlation and identifiability of parameters (Reactions 3 and 4) were determined using MCMC method, the parameters identified well, and no pathological cross-correlation could be seen between any parameter pair.

Keywords: Alumina, Butylbenzene, Chromia, Dehydrocyclization, Diester, Dimethylnaphthalene, Disproportionation, Esterification, Ethylhexanoic acid, HZSM-22, Isobutyric acid, MCMC, Methylbutene, Monoester, Naphthalene, Neopentyl glycol, Pentene, Propionic acid, Resin, Skeletal isomerization, 1-(*p*-Tolyl)-2-methylbutane
UDC 544.43 : 547 : 66.097.3

ACKNOWLEDGEMENTS

First of all I want to thank Prof. Matti Lindström and PhD Salme Koskimies, because they offered me chance to work with the projects on which my dissertation is based. My supervisors Prof. Heli Siren and Doc. Jaakko Partanen have revised the literature part of the dissertation, and I want to thank them about their advices and suggestions for the corrections.

As a project researcher, I cooperated with several individuals: Tech. Lic. Markku Laatikainen, MSc Kari-Matti Sahala, MSc Susanna Saukkonen, MSc Sylvie Maury and Mr. Olli Metsälä, to whom I am also very grateful for their contribution to the work.

Considering mathematical modeling I got valuable support from Doc. Arto Laari, MSc Antti Solonen, and Prof. Heikki Haario, to whom also I wish to express my sincere gratitude. Especially I want to thank Antti Solonen, who has checked the chapters that cover Markov chain Monte Carlo (MCMC) method.

In addition, I wish to thank the staff of the Department of LUT Chemistry for the support and cooperation and B.Sc. Peter Jones for revising the language of the publications I, IV, and V.

I am grateful for the reviewers Professors Andres Öpik and Marita Niemelä for their valuable comments on the thesis. These comments have helped me to improve its quality.

Lappeenranta, September 17, 2010

Kari Vahteristo

TABLE OF CONTENTS

LIST OF PUBLICATIONS

The thesis is based on the following five scientific publications. In the text these publications will be referred to by their roman numerals (I-V).

I Laatikainen, M., Vahteristo, K., Saukkonen, S., Lindström, M., Kinetics of *n*-Butylbenzene Dehydrocyclization over Chromia-Alumina. *Ind. Eng. Chem. Res. 35*, 2103–2109 (1996).

II Vahteristo, K., Sahala, K.-M., Koskimies S., Catalytic Studies toward Synthesis of 2,6-Dimethylnapththalene from 1-(*p*-Tolyl)-2-methylbutane. *Ind. Eng. Chem. Res. 49*, 4018–4025 (2010).

III Vahteristo, K., Laari, A., Haario, H., Solonen, A., Estimation of Kinetic Parameters in Neopentyl Glycol Esterification with Propionic Acid. *Chem. Eng. Sci. 63*, 587–598 (2008).

IV Vahteristo, K., Maury, S., Laari, A., Solonen, A., Haario, H., Koskimies, S., Kinetics of Neopentyl Glycol Esterification with Different Carboxylic Acids. *Ind. Eng. Chem. Res. 48*, 6237–6247 (2009).

V Vahteristo, K., Sahala K.-M., Laari, A., Solonen, A., Haario, H., Skeletal Isomerization Kinetics of 1-Pentene over H-ZSM-22 Catalyst. *Chem. Eng. Sci. 65*, 4640–4651 (2010).

Author's contribution

I Tech. Lic. Laatikainen has written the article together with the author. Reactor system has been constructed by the author. Paper was based on Miss Saukkonen's Master of Science thesis supervised by Laatikainen, the author, and Prof. Lindström.

II The author has written the article. Reactor systems have been constructed by the author. Experimental runs and analyses have been performed by the author and MSc Sahala. Modeling work has been performed by the author. Supervised by Doc. Koskimies.

III The author has written the article excluding the theory of the statistical treatment analysis. Experimental runs and analyses have been performed by the author. Modeling work has been performed by the author, Doc. Laari, MSc Solonen, and Prof. Haario.

IV The author has written the article excluding the theory of the statistical treatment analysis. Experimental runs and analyses have been performed by the author and by MSc Maury. Modeling work have been performed by the author, Solonen, and Laari. Supervised by Koskimies (experimental) and Haario (modeling).

V The author has written the article excluding the theory of the statistical treatment analysis. Reactor systems have been constructed by the author and by Sahala. Experimental runs and analyses have been performed by the author. Modeling work has been performed by the author, Solonen, and Laari. Supervised by Haario (modeling).

NOMENCLATURE

Symbols

A	pre-exponential factor, min^{-1}, kg mol^{-1} min^{-1}, mol kg^{-1} min^{-1}, mol g_C^{-1} s^{-1}
C	concentration of a component in organic phase, mol kg^{-1}(all components)
E	activation energy, J mol^{-1}
g	the observation function that maps the model state
K	equilibrium constant, -
k	apparent reaction rate constant, min^{-1}, kg mol^{-1} min^{-1}, mol kg^{-1} min^{-1}, mol g_C^{-1} s^{-1}
L	the likelihood
M	molar mass, kg^{-1} mol
m	mass, g
$\dot{m}$	mass flow rate, g h^{-1}
n	amount, mol
$\dot{n}$	molar flow rate, mol s^{-1}
p	partial pressure, kPa
p	the prior
p^{θ}	the standard pressure, 101.3 kPa
R	gas constant, 8.315 J K^{-1} mol^{-1}
R^2	the coefficient of determination, -
RSS	the sum of least squares in optimum
r	reaction rate, mol g_C^{-1} s^{-1}
s	the model state
SQ	the sum of least squares
T	temperature, K
t	time, s
w	mass fraction, -
WHSV	weight hourly space velocity, h^{-1}
x	mole fraction, -

x	the design variable
y	the response that is observed
y_p	the response that is calculated using the model
$\bar{y}$	the average value of all data points

α	apparent reaction order, -
ε	the experimental error
θ	the unknown parameter in the model
π	the posterior distribution
σ^2	variance

Abbreviations

ACID	carboxylic acid (PRO, IBA or EHA)
AE	dehydrogenation of 1-(*p*-tolyl)-2-methylbutane to –butene
AE	dehydrogenation of *n*-butylbenzene *n*-butenylbenzene
AF	1-(*p*-tolyl)-2-methylbutane fragmentation
AF	*n*-butylbenzene fragmentation
AI	1-(*p*-tolyl)-2-methylbutane 1,5-cyclization
AI	*n*-butylbenzene 1,5-cyclization
AN	*n*-butylbenzene 1,6-cyclization
AS	*n*-butylbenzene skeletal isomerization
BB	butylbenzene
BeB	butenylbenzenes
C	catalyst
D	dimerization products
DDD	dealkylation of 1,6-cyclization products
DEEHA	neopentyl glycol di-2-ethylhexanate
DEIBA	neopentyl glycol di-isobutyrate
DEPRO	neopentyl glycol dipropionate

DF	fragmentation of dimerization products
DMN	dimethylnaphthalene
DE	diester
EA	hydrogenation of 1-(*p*-tolyl)-2-methylbutene to –butane
EA	hydrogenation of *n*-butenylbenzene to *n*-butylbenzene
ED	1-(*p*-tolyl)-2-methylbutene 1,6-cyclization
EF	1-(*p*-tolyl)-2-methylbutene fragmentation
EF	*n*-butenylbenzene fragmentation
EHA	2-ethylhexanoic acid
EI	1-(*p*-tolyl)-2-methylbutene 1,5-cyclization
EI	*n*-butenylbenzene 1,5-cyclization
EN	*n*-butenylbenzene 1,6-cyclization
exp	experimental
fit	fitted
F	flow
F	fragmentation products
FID	flame ionization detector
FCC	fluid catalytic cracking
Fr	fragmentation products
GC	gas chromatograph
I	isopentenes
ID	dimerization of isopentenes
IP	skeletal isomerization of isopentenes
i	component, compound, moment
IBA	isobutyric acid
ID	dealkylation of 1,5-cyclization products
j	component, reaction
MB	1-(*p*-tolyl)-2-methylbutane
MBes	1-(*p*-tolyl)-2-methylbutene isomers
ME	monoester
mean	“mean” temperature value between the minimum and maximum used in the experiments

MEEHA	neopentyl glycol mono-2-ethylhexanate
MEIBA	neopentyl glycol monoisobutyrate
MEPRO	neopentyl glycol monopropionate
mix	mixture
MS	mass spectrometer
NDC	naphthalene-dicarboxylic acid
NPG	neopentyl glycol
P	*n*-pentenes
PD	dimerization of *n*-pentenes
PEN	poly(ethylene-2,6-naphthalene-dicarboxylate)
PI	skeletal isomerization of *n*-pentenes
PID	dimerization of *n*-pentenes with isopentenes
PRO	propionic acid
SI	skeletal isomerization products
TAEE	*tert*-amyl ethyl ether
TAME	*tert*-amyl methyl ether
TCD	thermal conductive detector
W	water
15	1,5-cyclization products
16	1,6-cyclization products

PART I: OVERVIEW OF THE DISSERTATION

1 INTRODUCTION

The aim of this thesis is to study reaction kinetics of four separate reactions:

1. Dehydrocyclization of *n*-butylbenzene (BB) to produce naphthalene

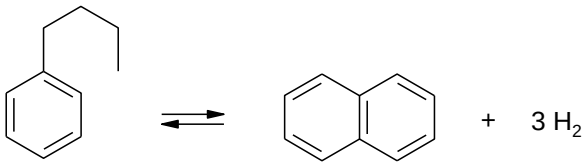

(1)

2. Dehydrocyclization of 1-(*p*-tolyl)-2-methylbutane (MB) to produce 2,6-dimethylnaphthalene (2,6-DMN)

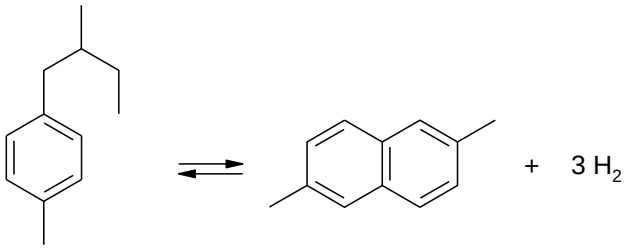

(2)

3. Esterification of neopentyl glycol (NPG) with different carboxylic acids to produce monoesters. In Reaction 3 propionic acid have been used for esterification.

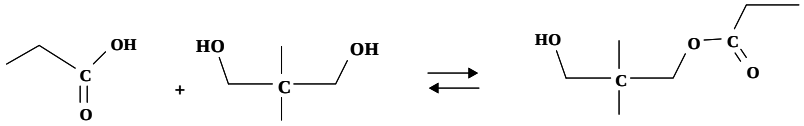

(3)

4. Skeletal isomerization of 1-pentene to produce 2-methyl-1-butene and 2-methyl-2-butene

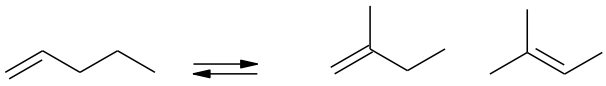

(4)

Reactions 1 and 2 have been studied, since 2,6-DMN is one of the most common reactants in the production of 2,6-naphthalene-dicarboxylic acid (2,6-NDC), the price of which affects strongly on the price of poly(ethylene-2,6-naphthalene-dicarboxylate) (PEN) (see Figure 1.1). PEN is an interesting polyester for industrial yarn and film applications, because some of its mechanical and barrier properties are better than those of the commonly used poly(ethyleneterephthalate) (PET) (Huijts and de Vries, 1993; Nakamura, 1992).

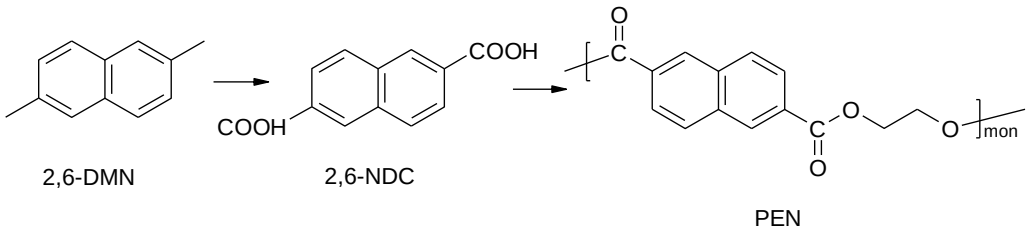

Figure 1.1 Reaction steps to produce PEN.

Reaction 1 has no commercial importance, while it is relevant as a model reaction because of the complexity of MB dehydrocyclization reaction. Furthermore it is easier and much cheaper to get synthetic BB than MB which make possible to perform several experiment in order to study the elementary steps of the dehydrocyclization process. Although dehydrocyclization of BB has been studied rather broadly in literature (Csicsery, 1967, 1968; Pines and Goetschel, 1966; Arnaudov and Dimitrov, 1969), the kinetics of the reactions involved is poorly understood. In this research, kinetics of BB dehydrocyclization over selfmade chromia-alumina –catalyst was studied in **I**. In addition, kinetics of MB dehydrocyclization over commercial chromia-alumina of different acidity, platina on silica, and vanadium/calcium/alumina was studied in **II**.

Reaction 3 has been selected due to its relevance in coating applications. Many synthetic polymer latexes (particularly acrylic and vinyl ester latexes) form films that have excellent physical and chemical properties. Unfortunately, many of these latexes have not desirable film forming properties in many conventional coating applications. Because of that it is a common practice to add a non-volatile plasticizer (such as alkyl phthalate esters or phosphate esters) to the latex. However, these plasticizers make films soft and tacky causing dirt accumulation and blocking

problems both during and after drying. In order to overcome these problems, it has become a common practice to add a fugitive coalescing agent to the latex. It has been found that aliphatic glycols, aliphatic glycol esters, aromatic glycol ethers, esters of phenol and acetate capped glycol ethers are acceptable as fugitive coalescing agents in most coating applications. It has been found that certain hydrolytically stable esters may function as coalescents and provide a desirable balance of block resistance and low temperature film formation (Friel, 1981). Esterification of NPG with isobutyric (IBA), propionic (PRO) (Reaction 3) or 2-ethylhexanoic (EHA) acid have been studied in **III** and **IV**. In these reactions gellular type resin (Dowex 50 WX 2), macroreticular type resin (Amberlyst 15) or *para*-toluene sulfonic acid in the same phase was used as a catalyst.

The great demand for branched ethers for high octane unleaded gasoline has created growing markets for oxygenate compounds, namely for TAEE (*tert*-amyl ethyl ether) and TAME (*tert*-amyl methyl ether). Skeletal isomerization of *n*-pentenes (Reaction 4) is an important reaction route to produce the raw material for TAME synthesis. It is based on the reaction between reactive isopentene compounds (2-methyl-1-butene and 2-methyl-2-butene) and methanol (Chase and Woods, 1979; Mooiweer *et al.*, 1994; Duplan *et al.*, 1996). Skeletal isomerization of 1-pentene over H-ZSM-22 –catalyst have been studied in **V**.

The successful integration of simulation tools requires the construction of sufficient databases of chemical kinetics and species information to allow broad application of these capabilities to real industrial processes. However, finding the reaction mechanisms in the literature are difficult, and they are often not in a form that can easily be used in a reactor simulation (Meeks, 2000). Therefore in this thesis, the experimental data with mechanistic view is integrated to modeling and simulation tools. The target is to construct sufficient databases containing chemical kinetics and species information to allow broad application of these tools to real industrial processes. This thesis fulfill in some extend the requirements of simulation tools concerning the studied reactions, because according to the fitting results, the suggested reaction mechanisms explain the experimental results rather well. When the possible cross-correlation and identifiability of parameters (Reactions 3 and 4) were determined using Markov chain Monte Carlo (MCMC) method, the parameters identified well, and no pathological cross-correlation could be seen between any parameter pair.

2 REACTIONS AND CATALYSTS

2.1 Dehydrocyclization of *n*-butylbenzene (BB)

Chromia/alumina -catalysts are highly porous, poorly crystallized, heterogeneous mixtures of various kinds of oxides of aluminium (Al_2O_3) and chromium (Cr_2O_3) (Poole and Mac Iver, 1967). The structures of these catalysts are of considerable complexity. Cr_2O_3/ Al_2O_3 can be regarded as a dual function catalyst possessing an acidic function which is primarily associated with the alumina phase and a dehydrogenation function which resides in the chromia phase. The former function is presumably responsible for reactions such as isomerization and cracking, while the latter catalyzes hydrogenation, dehydrogenation and aromatization reactions.

Because of the dual functionality, chromia/alumina is a suitable catalyst for examining 1,5- and 1,6-cyclization reactions when using *n*-butylbenzene as the reactant. 1,5-Cyclization can occur via two mechanisms: the first mechanism is catalyzed by the metal and the second by the acid sites. This is due to alumina that is capable of catalyzing reactions involving a carbonium ion intermediates. Naphthalene cannot be formed from *n*-butylbenzene by such a mechanism because the reaction would involve a very unstable primary carbonium ion (Csicsery, 1967).

Following reaction mechanism for *n*-butylbenzene over chromia/alumina can be considered (**I**, Scheme 1, Figure 2.1)

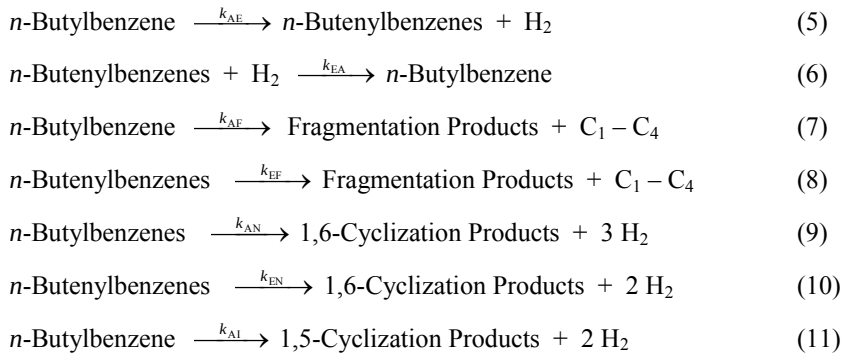

$$n\text{-Butenylbenzenes} \xrightarrow{k_{EI}} \text{1,5-Cyclization Products} + H_2 \quad (12)$$

$$n\text{-Butylbenzene} \xrightarrow{k_{AS}} \text{Skeletal Isomerization Products} \quad (13)$$

$$\text{1,5-Cyclization Products} \xrightarrow{k_{ID}} \text{Dealkylation Products} \quad (14)$$

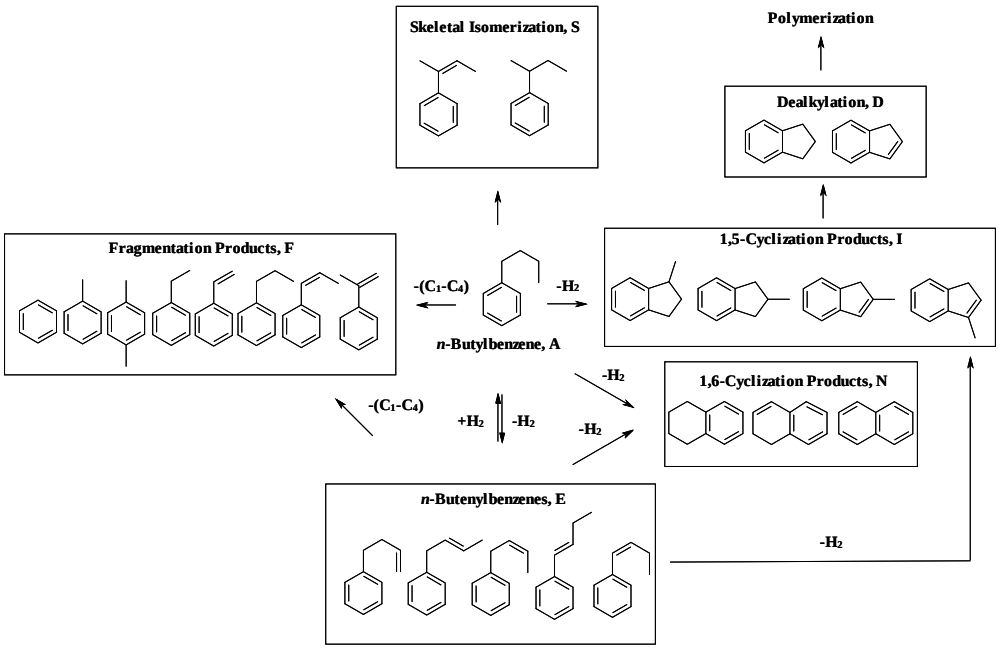

Figure 2.1 Steps in the reaction mechanism for *n*-butylbenzene over chromia/alumina (**I**, Scheme 1).

According to the performed experiments, fragmentation products were mainly toluene, ethylbenzene, styrene and propylbenzene. Fragmented gaseous products (C_1 – C_4) were methane, ethane, ethylene, propane, propylene, *n*-butane, *trans*-2-butene, *cis*-2-butene, 1-butene and isobutylene. The 1,5- and 1,6-cyclization products were methylindanes, –indenes and naphthalene, respectively. Skeletal isomerization products were isobutyl- and isobutenylbenzene. Dealkylation produced indane and indene. In all experiments, different *n*-butenylbenzene isomers reached the chemical equilibrium and the compositions agreed rather well at those states with the literature values (Csicsery, 1968).

2.2 Dehydrocyclization of 1-(p-tolyl)-2-methylbutane (MB)

When producing a reactant for a dehydrocyclization reaction aiming to produce 2,6-DMN, it is necessary to prepare alkylbenzene that has a side chain longer than three carbon atoms. It is common to use xylene as a reactant (Taniguchi and Matsuoka, 1975; Abe, T., Ebata, S. *et al.*, 1990; Shimada, 1993) to make alkylation with olefins or diolefins over a specific alkali metal as the catalyst. In addition, toluene (Abe, T., Uchiyama, S. *et al.*, 1990) and 2,4,6-octatriene (Miyamoto *et al.*, 1973) have been used as the starting material for the reaction. When producing 1-(*p*-tolyl)-2-methylbutane or –butenes and using *p*-xylene and butenes or butadiene as reactants, especially alkali metals such as sodium, potassium and rubidium are preferred as catalysts (Mitsui Petrochemical Industries Ltd, 1973; Kiricsi *et al.*, 1997).

When C_{12}-butyl- and butenylbenzenes are heated in the presence of a cyclization-dehydrogenation catalyst, both cyclization and dehydrogenation proceed concurrently. Depending on the position of the pendant methyl group, the product is 1,5-, 1,6-, 2,6- or 2,7-dimethylnaphthalene (Mitsui Petrochemical Industries Ltd, 1973; Shimada., 1993). 1-(*p*-Tolyl)-2-methylbutenes (MBes) contain 6 isomers depending on the double bond position and molecular geometry related to *cis* and *trans* isomerization (Inamasi *et al.*, 1993). Any of these isomers alone or in the form of mixture may be used in the main reaction (**II**, p. 4018).

Following reaction mechanism for MB dehydrocyclization and its side reactions can be considered

$$\text{MB} \xrightarrow{k_{AE}} \text{MBes} + \text{H}_2 \quad (15)$$

$$\text{MBes} + \text{H}_2 \xrightarrow{k_{EA}} \text{MB} \quad (16)$$

$$\text{MB} \xrightarrow{k_{AF}} \text{Fragmentation Products} + \text{C}_1 - \text{C}_4 \quad (17)$$

$$\text{MBes} \xrightarrow{k_{EF}} \text{Fragmentation Products} + \text{C}_1 - \text{C}_4 \quad (18)$$

$$\text{MBes} \xrightarrow{k_{ED}} \text{1,6-Cyclization Products} + 2\,\text{H}_2 \quad (19)$$

$$\text{MB} \xrightarrow{k_{AI}} \text{1,5-Cyclization Products} + 2\,\text{H}_2 \quad (20)$$

$$\text{MBes} \xrightarrow{k_{EI}} \text{1,5-Cyclization Products} + \text{H}_2 \quad (21)$$

$$\text{1,5-Cyclization Products} \xrightarrow{k_{ID}} \text{Dealkylation Products} \quad (22)$$

$$\text{1,6-Cyclization Products} \xrightarrow{k_{DDD}} \text{Dealkylated 1,6-Cyclization Products} \quad (23)$$

Fragmentation products were mainly *p*-xylene and 3-(*p*-tolyl)-propylenes, 1,5-cyclization products were trimethylindanes and –indenes, and 1,6-cyclization products were dimethylnaphthalenes. Dealkylated 1,6-cyclization products were 2-methylnaphthalene and naphthalene. Fragmented gaseous products (C_1 – C_4) were methane, ethane, ethene, propane, propene, *n*-butane, *trans*-2-butene, *cis*-2-butene, 1-butene, and isobutylene (**II**, Figure 1).

2.3 Esterification of neopentyl glycol (NPG) with different carboxylic acids

The esterification reaction is a broadly researched and applied process, that usually attains the equilibrium. Typically the equilibrium constant for esterification reactions has a value from 1 to 10 (Rönnback *et al.*, 1997). When glycol reacts with an organic acid, the products are monoester and water. Monoester reacts further with the organic acid forming diester (Astle, 1955). Normally water is distilled during a process in order to shift reaction equilibrium towards the products (Rönnback *et al.*, 1997). Minor reaction in the process is disproportionation (as observed in **III** and **IV**), which is harmful, particularly during separation, because it reduces the amount of monoester which is normally the desired product (**III**, p. 587).

Reaction mechanism for esterification of NPG with a carboxylic acid can be written

$$\text{NPG} + \text{Acid} \xrightarrow{k_1} \text{Monoester} + H_2O \quad (24)$$

$$\text{Monoester} + \text{Acid} \xrightarrow{k_2} \text{Diester} + H_2O \quad (25)$$

$$\text{Diester} + \text{NPG} \xrightarrow{k_3} 2\ \text{Monoester} \quad (26)$$

$$2\ \text{Monoester} \xrightarrow{k_{-3}} \text{Diester} + \text{NPG} \quad (27)$$

When using propionic (PRO), isobutyric (IBA) or 2-ethylhexanoic acid (EHA), the monoesters were neopentyl glycol monopropionate (MEPRO), neopentyl glycol monoisobutyrate (MEIBA) or neopentyl glycol mono-2-ethylhexanate (MEEHA). Diesters were neopentyl glycol dipropionate

(DEPRO), neopentyl glycol di-isobutyrate (DEIBA) and neopentyl glycol di-2-ethylhexanate (DEEHA), respectively.

Esterification reactions were usually catalysed by mineral acids, but nowadays ion exchange resins have gained prominence as catalysts. Their advantages are numerous when compared to mineral acids: freedom from corrosive action, easy removal of the catalyst, and comparatively mild conditions of reaction (Bhagade and Nageshwar, 1978). The resins typically employed are sulfonic acid cation exchangers or quaternary ammonium anion exchangers in the hydroxide form. The resins can be divided into the following two groups on the basis of their structural differences: gel and macroreticular resins (Chakrabarti and Sharma, 1993). The swelling ability of the reactants is a prerequisite for catalysis by gel resins, but macroreticular resins may also function in non-swelling solvents. The selectivity of ion exchanger catalysts often leads to yields which are considerably higher than those obtained with catalysis by dissolved electrolytes (Chakrabarti and Sharma, 1993; Helfferich, 1962). The esterification of carboxylic acid with olefins in the presence of cation-exchange resins has considerable academic and industrial importance (Saha and Sharma, 1996). Their use both as a catalyst and a selective sorbent in a continuous chromatographic reactors has been studied (Mazzotti *et al.*, 1996; Mazzotti *et al.*, 1997). Furthermore, their use as a catalyst for fuel oxygenation agent production have been thoroughly researched (Fité *et al.*, 1994; Parra *et al.*, 1998; Rehfinger and Hoffman, 1990).

2.4 Skeletal isomerization of 1-pentene

Isomerization mechanisms of linear olefins are based on the reaction of carbenium ions. It has been shown that alkenes are adsorbed at Brønsted sites on solid acid catalysts to produce carbenium ions (Abbot and Wojciechowski, 1988). A carbenium ion reaction occurs as a rearrangement through hydrogen-atom or carbon-atom shift. The former mechanism leads to a double-bond or *cis-trans* isomerization and the latter to the skeletal rearrangement of the olefin (Gates, 1979). In addition, dimerization and cracking reactions are assumed to be carbenium ion catalyzed. The carbenium ion is assumed to be formed on Brønsted acid sites (Cheng and Ponec, 1994) (**V**, p. 4640).

When isomerizing *n*-pentene over ZSM-5 catalyst three possible skeletal isomers were found: 2-methyl-1-butene, 2-methyl-2-butene, and 3-methyl-1-butene (Abbot and Wojciechowski, 1985). Monomolecular cracking process did not occur, and primary C_3 and C_4 fragments formed via the dimerization-cracking mechanism (Abbot and Wojciechowski, 1985; Zhang, 1995). Oligomerization was limited to dimer formation (Abbot and Wojciechowski, 1985).

The possible reaction mechanism for 1-pentene skeletal isomerization can be considered as follows

$$n\text{-Pentenes} \xrightarrow{k_{PI}} \text{Isopentenes} \quad (28)$$

$$\text{Isopentenes} \xrightarrow{k_{IP}} n\text{-Pentenes} \quad (29)$$

$$2\ n\text{-Pentenes} \xrightarrow{k_{PD}} \text{Dimerization Products} \quad (30)$$

$$2\ \text{Isopentenes} \xrightarrow{k_{ID}} \text{Dimerization Products} \quad (31)$$

$$n\text{-Pentenes} + \text{Isopentenes} \xrightarrow{k_{PID}} \text{Dimerization Products} \quad (32)$$

$$\text{Dimerization Products} \xrightarrow{k_{DF}} 2\ \text{Fragmentation Products} \quad (33)$$

n-Pentenes included 1-pentene and *cis*- and *trans*-2-pentenes and isopentenes were 2-methyl-1-butene, 2-methyl-2-butene, and 3-methyl-1-butene. Dimerization products were C_{10} –alkanes and –alkenes, and fragmentation products were C_2, C_3, C_4, C_6, C_7, C_8 -alkanes and –alkenes.

ZSM-22 zeolite based catalyst possesses good shape-selective properties for iso-olefin production and it has been widely used as the catalyst for skeletal isomerization of the C_4 fraction (Bäck and Lee, 1997; Houžvicka *et al.*, 1997; Byggningsbacka *et al.*, 1997 and 1998; Simon *et al.*, 1994). ZSM-22 has a theta-1 type structure and it consists of single rings and an unidirectional and one-dimensional 10-membered tetrahedral ring channel system (5.5 × 4.5 Å) (Simon *et al.*, 1994; Meier and Olson; 1987). The Si/Al ratio of ZSM-22 is high (45) (Simon *et al.*, 1994) and a Brønsted to Lewis acid ratio is 7.0 according to pyridine adsorption data (Simon *et al.*, 1994) (**V**, p. 4641).

3 EXPERIMENTAL

A detailed description of the materials, devices, catalyst treatments, product analyses, and procedures to perform analyses and experiments has been given in **I**, **II**, **III**, **IV** and **V**.

3.1 Dehydrocyclization of BB and MB

Experimental data were obtained by means of a standard isothermal fixed bed tube reactor. Detailed figure about apparatus has been published previously (Saukkonen, 1995; Vahteristo *et al.*, 1996). BB dehydrocyclization experiments were performed with a self-prepared Cr_2O_3/Al_2O_3 -catalyst. When using MB as a reactant, several catalysts were studied: a commercial Cr_2O_3/Al_2O_3, a potassium impregnated Cr_2O_3/Al_2O_3 (potassium content of 4.7 wt-%), Pt/SiO_2, and V/Ca/ Al_2O_3. The liquid samples were analyzed using a HP 5890 Series II Plus gas chromatograph (GC) with a crosslinked phenyl methyl silicone capillary column (HP-5, 19091J-413). To analyze 2,6-DMN and 2,7-DMN, a polarized column (biscyanol phenylcyanopropyl polysiloxane, J&W Scientific, DB-DXN P/N 122-2461) had to be used, because non-polar column (HP-5) was not able to separate these components. The gaseous reaction products were analyzed using GC with a capillary column (HP-PLOT/Al_2O_3, 19035P-323). The injector was split/splitless and the detector was a flame ionization detector (FID). Few liquid samples were analyzed with GC-mass spectrometer (MS) (JEOL JMS-AX505WA, HP-5) and the identification of liquid compounds based mainly on these analyses (**I**, p. 2103-2104; **II**, p. 4018-4019).

3.2 Esterification of NPG with different carboxylic acids

Experiments were performed in a 650 ml glass batch reactor (**III**, p. 588) under isothermal conditions. A commercial *para*-toluenesulfonic acid, a gellular type resin (Dowex 50WX2) and a macroreticular type resin (Amberlyst 15) were used as catalysts. Experiments without a catalyst were also performed. The liquid samples were analyzed using a HP 5890 Series II Plus GC. The injector was split/splitless. The peaks of NPG, PRO, IBA, EHA, and their corresponding

monoesters and diesters were identified by comparing with pure components, which were also used for the calculation of the response factors. These monoesters and diesters were got by distilling a product mixture for disproportionation experiments using a spinning band distillation column. Reactants and products were analyzed with FID using a cross-linked methyl siloxane capillary column (HP-1MS, 19091S-933, 30 m). Some samples were analyzed before dilution with a thermal conductive detector (TCD) in order to clarify the amount of water in the product mixture. These analyses were performed with a crosslinked methyl silicone gum capillary column (HP-1, 19091Z-236, 60 m) (**IV**, p. 6238–6239).

3.3 Skeletal isomerization of 1-pentene

Skeletal isomerization experiments were carried out in a standard isothermal fixed bed reactor system using HZSM-22 as a catalyst. At the end of each run, the deactivated catalyst was regenerated by a controlled burn sequence with nitrogen diluted air. After 43 regenerations and over 500 h on-stream, the catalyst remained active. The reaction products were analyzed on-line by means of GC (HP 5890 Series II Plus) with a crosslinked methyl siloxane capillary column (HP-1, 19091Z-236, 60 m). The injector was split/splitless, and the detector was FID. The GC-analysis calibration table was prepared based on peak identification results with GC-MS by NESTE Company and Lappeenranta University of Technology (JEOL JMS-AX505WA, HP-1, 19091Z-236, 60 m) (**V**, p. 4641).

4 KINETIC MODELING

4.1 Dehydrocyclization of BB

Reactions of *n*-butylbenzene were modeled using a pseudohomogeneous model with the reaction mechanism presented in Reactions 5–14. Kinetic parameters were fitted using experimental data determined for *n*-butylbenzene and for groups of *n*-butenylbenzenes, fragmentation products, 1,6-cyclization products, 1,5-cyclization products, and skeletal isomerization products. The amount of hydrogen and C_1–C_4 gases were calculated stoichiometrically. In order to simplify the task, the reaction orders have been taken from initial-rate data (as presented in **I**).

The apparent reaction rate constants and orders based on initial-rate experiments were determined using the following rate law

$$r_j = \frac{d\dot{n}_j}{dm_C} = k_j \prod_i \left(\frac{p_i}{p^\theta} \right)^{\alpha_{j,i}} \tag{4.1}$$

where: r_j the reaction rate for a component *j*
p_i partial pressure of component *i*
p^θ the standard pressure (101.3 kPa)
k_j apparent reaction rate constant for production of component *j*
$\dot{n}_j$ molar flow rate of a component *j*
m_c the mass of the catalyst
$\alpha_{j,i}$ apparent reaction order, i refers to component and *j* to reaction (see Figure 2.1)

Weight hourly space velocity (WHSV) is defined in Equation 4.2.

$$\text{WHSV} = \frac{\dot{m}_F}{m_C} \tag{4.2}$$

where: $\dot{m}_F$ mass flow rate of a reactant

When WHSV is taken inverse and both parts of equation is derived assuming that $\dot{m}_F$ is constant, Equation 4.3 can be written.

$$dm_C = \dot{m}_F d(1/\mathrm{WHSV}) \tag{4.3}$$

Differential equations for reaction mechanism (Reactions 5–14) can be written by using Equation 4.1 for an individual reaction in the mechanism. If dm_c in Equation 4.1 is replaced using Equation 4.3 Equations 4.4–4.10 can be written. Reaction orders are as those determined for temperature of 783 K (in **I**).

$$\frac{1}{\dot{m}_F}\frac{d\dot{n}_{BB}}{d(1/\mathrm{WHSV})} = -k_{AE}\left(\frac{p_{BB}}{p^\theta}\right)^{0.53} + k_{EA}\left(\frac{p_{BeB}}{p^\theta}\right)^{0.8}\left(\frac{p_H}{p^\theta}\right)^{0.1} - k_{AN}\left(\frac{p_{BB}}{p^\theta}\right)^{0.75} - k_{AF}\left(\frac{p_{BB}}{p^\theta}\right)^{1.1} - k_{AI}\left(\frac{p_{BB}}{p^\theta}\right)^{0.18} - k_{AS}\left(\frac{p_{BB}}{p^\theta}\right) \tag{4.4}$$

$$\frac{1}{\dot{m}_F}\frac{d\dot{n}_{BeB}}{d(1/\mathrm{WHSV})} = k_{AE}\left(\frac{p_{BB}}{p^\theta}\right)^{0.53} - k_{EA}\left(\frac{p_{BeB}}{p^\theta}\right)^{0.8}\left(\frac{p_H}{p^\theta}\right)^{0.1} - k_{EF}\left(\frac{p_{BeB}}{p^\theta}\right)^{1.1} - k_{EN}\left(\frac{p_{BeB}}{p^\theta}\right)^{1.5} - k_{EI}\left(\frac{p_{BeB}}{p^\theta}\right)^{1.1} \tag{4.5}$$

$$\frac{1}{\dot{m}_F}\frac{d\dot{n}_{Fr}}{d(1/\mathrm{WHSV})} = k_{AF}\left(\frac{p_{BB}}{p^\theta}\right)^{1.1} + k_{EF}\left(\frac{p_{BeB}}{p^\theta}\right)^{1.1} \tag{4.6}$$

$$\frac{1}{\dot{m}_F}\frac{d\dot{n}_{16}}{d(1/\mathrm{WHSV})} = k_{AN}\left(\frac{p_{BB}}{p^\theta}\right)^{0.75} + k_{EN}\left(\frac{p_{BeB}}{p^\theta}\right)^{1.5} \tag{4.7}$$

$$\frac{1}{\dot{m}_F}\frac{d\dot{n}_{15}}{d(1/\mathrm{WHSV})} = k_{AI}\left(\frac{p_{BB}}{p^\theta}\right)^{0.18} + k_{EI}\left(\frac{p_{BeB}}{p^\theta}\right)^{1.1} - k_{ID}\left(\frac{p_{15}}{p^\theta}\right)^{1.4} \tag{4.8}$$

$$\frac{1}{\dot{m}_F}\frac{d\dot{n}_{SI}}{d(1/\mathrm{WHSV})} = k_{AS}\left(\frac{p_{BB}}{p^\theta}\right) \tag{4.9}$$

$$\frac{1}{\dot{m}_{\mathrm{F}}}\frac{d\dot{n}_{\mathrm{H}}}{d(1/\,\mathrm{WHSV}\,)} = r_{\mathrm{BeB}} + 2r_{15} + 2.5r_{16} \tag{4.10}$$

The kinetic model formed by Equations 4.4 to 4.10 has 10 apparent reaction rate constants, which are k_{AE}, k_{EA}, k_{AI}, k_{EI}, k_{AN}, k_{EN}, k_{AF}, k_{EF}, k_{ID}, and k_{AS}.

The temperature dependence of the apparent reaction rate constants is expressed by the Arrhenius law

$$k_j = A\exp\left(-\frac{E}{RT}\right) \tag{4.11}$$

where: A pre-exponential factor
E activation energy
R gas constant
T temperature

Equation 4.11 was linearized and parameters of this Arrhenius law were estimated using linear regression analysis.

4.2 Dehydrocyclization of MB

Reactions of MB were modeled using a pseudohomogeneous model with the reaction mechanism presented in Reactions 15–23. Kinetic parameters were fitted using experimental data determined for MB and for groups of MBes, fragmentation products, 1,6-cyclization products, 1,5-cyclization products, and dealkylated 1,6-cyclization products. The amount of hydrogen and C_1–C_4 gases were calculated stoichiometrically. In order to simplify the task, the reaction orders have been taken from initial-rate data of *n*-butylbenzene at 783 K (**I**).

Differential equations for reaction mechanism of Reactions 15–23 can be written by using Equation 4.1 for an individual reaction in the mechanism.

$$\frac{1}{\dot{m}_{\mathrm{F}}}\frac{d\dot{n}_{\mathrm{MB}}}{d(1/\mathrm{WHSV})} = -k_{\mathrm{AE}}\left(\frac{p_{\mathrm{MB}}}{p^{\theta}}\right)^{0.53} + k_{\mathrm{EA}}\left(\frac{p_{\mathrm{MBes}}}{p^{\theta}}\right)^{0.8}\left(\frac{p_{\mathrm{H}}}{p^{\theta}}\right)^{0.1} - k_{\mathrm{AF}}\left(\frac{p_{\mathrm{MB}}}{p^{\theta}}\right)^{1.1} - k_{\mathrm{AI}}\left(\frac{p_{\mathrm{MB}}}{p^{\theta}}\right)^{0.18} \quad (4.12)$$

$$\frac{1}{\dot{m}_{\mathrm{F}}}\frac{d\dot{n}_{\mathrm{MBes}}}{d(1/\mathrm{WHSV})} = k_{\mathrm{AE}}\left(\frac{p_{\mathrm{MB}}}{p^{\theta}}\right)^{0.53} - k_{\mathrm{EA}}\left(\frac{p_{\mathrm{MBes}}}{p^{\theta}}\right)^{0.8}\left(\frac{p_{\mathrm{H}}}{p^{\theta}}\right)^{0.1} - k_{\mathrm{EF}}\left(\frac{p_{\mathrm{MBes}}}{p^{\theta}}\right)^{1.1} - k_{\mathrm{ED}}\left(\frac{p_{\mathrm{MBes}}}{p^{\theta}}\right)^{1.5} - k_{\mathrm{EI}}\left(\frac{p_{\mathrm{MBes}}}{p^{\theta}}\right)^{1.1} \quad (4.13)$$

$$\frac{1}{\dot{m}_{\mathrm{F}}}\frac{d\dot{n}_{\mathrm{Fr}}}{d(1/\mathrm{WHSV})} = k_{\mathrm{AF}}\left(\frac{p_{\mathrm{MB}}}{p^{\theta}}\right)^{1.1} + k_{\mathrm{EF}}\left(\frac{p_{\mathrm{MBes}}}{p^{\theta}}\right)^{1.1} \quad (4.14)$$

$$\frac{1}{\dot{m}_{\mathrm{F}}}\frac{d\dot{n}_{16}}{d(1/\mathrm{WHSV})} = k_{\mathrm{ED}}\left(\frac{p_{\mathrm{MBes}}}{p^{\theta}}\right)^{1.5} - k_{\mathrm{DDD}}\left(\frac{p_{16}}{p^{\theta}}\right) \quad (4.15)$$

$$\frac{1}{\dot{m}_{\mathrm{F}}}\frac{d\dot{n}_{15}}{d(1/\mathrm{WHSV})} = k_{\mathrm{AI}}\left(\frac{p_{\mathrm{MB}}}{p^{\theta}}\right)^{0.18} + k_{\mathrm{EI}}\left(\frac{p_{\mathrm{MBes}}}{p^{\theta}}\right)^{1.1} - k_{\mathrm{ID}}\left(\frac{p_{15}}{p^{\theta}}\right)^{1.4} \quad (4.16)$$

$$\frac{1}{\dot{m}_{\mathrm{F}}}\frac{d\dot{n}_{16\mathrm{D}}}{d(1/\mathrm{WHSV})} = k_{\mathrm{DDD}}\left(\frac{p_{16}}{p^{\theta}}\right) \quad (4.17)$$

$$\frac{1}{\dot{m}_{\mathrm{F}}}\frac{d\dot{n}_{\mathrm{H}}}{d(1/\mathrm{WHSV})} = r_{\mathrm{MBes}} + 2r_{15} + 2.5r_{16} \quad (4.18)$$

The kinetic model formed by Equations 4.12 to 4.18 has 9 apparent reaction rate constants, which are k_{AE}, k_{EA}, k_{AF}, k_{EF}, k_{AI}, k_{EI}, k_{ED}, k_{DDD}, and k_{ID}.

4.3 Esterification of NPG with different carboxylic acids

Reactions of NPG with different carboxylic acids (PRO, IBA, EHA) were modeled using a pseudohomogeneous model with the reaction mechanism presented in Reactions 24–27. Kinetic parameters were fitted using experimental data determined for NPG, carboxylic acid, monoester and diester. Water was removed during measurements from the reactor using nitrogen flow.

Using a batch reactor model, the production rate for each component can be calculated from Equations 4.19–4.23.

$$r_{\mathrm{NPG}} = \frac{dC_{\mathrm{NPG}}}{dt} = -k_1 C_{\mathrm{NPG}} C_{\mathrm{ACID}} + k_{-1} C_{\mathrm{ME}} C_{\mathrm{W}} - k_3 C_{\mathrm{DE}} C_{\mathrm{NPG}} + k_{-3} C_{\mathrm{ME}}^2 \tag{4.19}$$

$$r_{\mathrm{ACID}} = \frac{dC_{\mathrm{ACID}}}{dt} = -k_1 C_{\mathrm{NPG}} C_{\mathrm{ACID}} + k_{-1} C_{\mathrm{ME}} C_{\mathrm{W}} - k_2 C_{\mathrm{ME}} C_{\mathrm{ACID}} + k_{-2} C_{\mathrm{DE}} C_{\mathrm{W}} \tag{4.20}$$

$$r_{\mathrm{ME}} = \frac{dC_{\mathrm{ME}}}{dt} = k_1 C_{\mathrm{NPG}} C_{\mathrm{ACID}} - k_{-1} C_{\mathrm{ME}} C_{\mathrm{W}} - k_2 C_{\mathrm{ME}} C_{\mathrm{ACID}} + k_{-2} C_{\mathrm{DE}} C_{\mathrm{W}} + 2k_3 C_{\mathrm{DE}} C_{\mathrm{NPG}} - 2k_{-3} C_{\mathrm{ME}}^2 \tag{4.21}$$

$$r_{\mathrm{DE}} = \frac{dC_{\mathrm{DE}}}{dt} = k_2 C_{\mathrm{ME}} C_{\mathrm{ACID}} - k_{-2} C_{\mathrm{DE}} C_{\mathrm{W}} - k_3 C_{\mathrm{DE}} C_{\mathrm{NPG}} + k_{-3} C_{\mathrm{ME}}^2 \tag{4.22}$$

$$r_{\mathrm{W}} = \frac{dC_{\mathrm{W}}}{dt} = k_1 C_{\mathrm{NPG}} C_{\mathrm{ACID}} - k_{-1} C_{\mathrm{ME}} C_{\mathrm{W}} + k_2 C_{\mathrm{ME}} C_{\mathrm{ACID}} - k_{-2} C_{\mathrm{DE}} C_{\mathrm{W}} \tag{4.23}$$

where: r the reaction rate
C the concentration of a component in organic phase using the unit of mol kg^{-1}
k the apparent reaction rate constant
t time

ACID refers to PRO, IBA or EHA. ME and DE refer to the corresponding monoester or diester.

As a result of continuous water removal, the amount of the reaction mixture decreases during the experiments. The amount of NPG is obtained from

$$n_{\mathrm{NPG}} = C_{\mathrm{NPG}} m_{\mathrm{mix}} \tag{4.24}$$

where: n the amount
m_{mix} the weight of the reaction mixture.

If Equation 4.24 is differentiated

$$dn_{\mathrm{NPG}} = m_{\mathrm{mix}}\, dC_{\mathrm{NPG}} + C_{\mathrm{NPG}}\, dm_{\mathrm{mix}} \tag{4.25}$$

and both parts of Equation 4.25 are divided by the time differential, Equation 4.26 is obtained.

$$\frac{dn_{\mathrm{NPG}}}{dt} = m_{\mathrm{mix}}\, \frac{dC_{\mathrm{NPG}}}{dt} + C_{\mathrm{NPG}}\, \frac{dm_{\mathrm{mix}}}{dt} \tag{4.26}$$

Assuming that the concentration of water in the reactor is negligible, Equation 4.19 for the molar reaction rate of NPG can be written as

$$\frac{dC_{\mathrm{NPG}}}{dt} = -k_1 C_{\mathrm{NPG}} C_{\mathrm{ACID}} - k_3 C_{\mathrm{DE}} C_{\mathrm{NPG}} + k_{-3} C_{\mathrm{ME}}^2 \tag{4.27}$$

Multiplying Equation 4.27 by m_{mix} obtains

$$\frac{dn_{\mathrm{NPG}}}{dt} = \left(-k_1 C_{\mathrm{NPG}} C_{\mathrm{ACID}} - k_3 C_{\mathrm{DE}} C_{\mathrm{NPG}} + k_{-3} C_{\mathrm{ME}}^2\right) m_{\mathrm{mix}} \tag{4.28}$$

Combining Equations. 4.28 and 4.26 gives

$$m_{\mathrm{mix}}\, \frac{dC_{\mathrm{NPG}}}{dt} + C_{\mathrm{NPG}}\, \frac{dm_{\mathrm{mix}}}{dt} = \left(-k_1 C_{\mathrm{NPG}} C_{\mathrm{ACID}} - k_3 C_{\mathrm{DE}} C_{\mathrm{NPG}} + k_{-3} C_{ME}^2\right) m_{\mathrm{mix}} \tag{4.29}$$

After rearrangement

$$\frac{dC_{\mathrm{NPG}}}{dt} = -k_1 C_{\mathrm{NPG}} C_{\mathrm{ACID}} - k_3 C_{\mathrm{DE}} C_{\mathrm{NPG}} + k_{-3} C_{\mathrm{ME}}^2 - \frac{C_{\mathrm{NPG}}}{m_{\mathrm{mix}}}\, \frac{dm_{\mathrm{mix}}}{dt} \tag{4.30}$$

By adapting Equations 4.24–4.26, 4.28 and 4.30 for each component, Equations.4.19–4.22 can be written as

$$r_{\mathrm{NPG}} = \frac{dC_{\mathrm{NPG}}}{dt} = -k_1 C_{\mathrm{NPG}} C_{\mathrm{ACID}} - k_3 C_{\mathrm{DE}} C_{\mathrm{NPG}} + k_{-3} C_{\mathrm{ME}}^2 - \frac{C_{\mathrm{NPG}}}{m_{\mathrm{mix}}}\, \frac{dm_{\mathrm{mix}}}{dt} \tag{4.31}$$

$$r_{\mathrm{ACID}} = \frac{dC_{\mathrm{ACID}}}{dt} = -k_1 C_{\mathrm{NPG}} C_{\mathrm{ACID}} - k_2 C_{\mathrm{ME}} C_{\mathrm{ACID}} - \frac{C_{\mathrm{ACID}}}{m_{\mathrm{mix}}}\, \frac{dm_{\mathrm{mix}}}{dt} \tag{4.32}$$

$$r_{\mathrm{ME}} = \frac{dC_{\mathrm{ME}}}{dt} = k_1 C_{\mathrm{NPG}} C_{\mathrm{ACID}} - k_2 C_{\mathrm{ME}} C_{\mathrm{ACID}} + 2k_3 C_{\mathrm{NPG}} C_{\mathrm{DE}} - 2k_{-3} C_{\mathrm{ME}}^2 - \frac{C_{\mathrm{ME}}}{m_{\mathrm{mix}}}\, \frac{dm_{\mathrm{mix}}}{dt} \tag{4.33}$$

$$r_{\mathrm{DE}} = \frac{dC_{\mathrm{DE}}}{dt} = k_2 C_{\mathrm{ME}} C_{\mathrm{ACID}} - k_3 C_{\mathrm{NPG}} C_{\mathrm{DE}} + k_{-3} C_{\mathrm{ME}}^2 - \frac{C_{\mathrm{DE}}}{m_{\mathrm{mix}}}\, \frac{dm_{\mathrm{mix}}}{dt} \tag{4.34}$$

Multiplying Equation 4.23 by m_{mix} gives Equations 4.35 and 4.36. The concentration of water in the reactor is assumed to be negligible.

$$r_{\mathrm{W}} m_{\mathrm{mix}} = \frac{dn_{\mathrm{W}}}{dt} = (k_1 C_{\mathrm{NPG}} C_{\mathrm{ACID}} + k_2 C_{\mathrm{ME}} C_{\mathrm{ACID}})\, m_{\mathrm{mix}} \tag{4.35}$$

$$\frac{dm_{\mathrm{mix}}}{dt} = -M_{\mathrm{W}} \frac{dn_{\mathrm{W}}}{dt} = -r_{\mathrm{W}} m_{\mathrm{mix}} M_{\mathrm{W}} \tag{4.36}$$

where: M_{W} the molar mass of water.

Then Equation 4.36 can be used to evaluate the decrease of the mass of the reaction mixture in Equations 4.31 to 4.34. Combining Equation 4.36 with Equation 4.31 the Equation 4.37 is obtained

$$r_{\mathrm{NPG}} = \frac{dC_{\mathrm{NPG}}}{dt} = -k_1 C_{\mathrm{NPG}} C_{\mathrm{ACID}} - k_3 C_{\mathrm{DE}} C_{\mathrm{NPG}} + k_{-3} C_{\mathrm{ME}}^2 + r_{\mathrm{W}} M_{\mathrm{W}} C_{\mathrm{NPG}} \tag{4.37}$$

Equations 4.32–4.34 may be rewritten similarly

$$r_{\mathrm{ACID}} = \frac{dC_{\mathrm{ACID}}}{dt} = -k_1 C_{\mathrm{NPG}} C_{\mathrm{ACID}} - k_2 C_{\mathrm{ME}} C_{\mathrm{ACID}} + r_{\mathrm{W}} M_{\mathrm{W}} C_{\mathrm{ACID}} \tag{4.38}$$

$$r_{\mathrm{ME}} = \frac{dC_{\mathrm{ME}}}{dt} = k_1 C_{\mathrm{NPG}} C_{\mathrm{ACID}} - k_2 C_{\mathrm{ME}} C_{\mathrm{ACID}} + 2k_3 C_{\mathrm{NPG}} C_{\mathrm{DE}} - 2k_{-3} C_{\mathrm{ME}}^2 + r_{\mathrm{W}} M_{\mathrm{W}} C_{\mathrm{ME}} \tag{4.39}$$

$$r_{\mathrm{DE}} = \frac{dC_{\mathrm{DE}}}{dt} = k_2 C_{\mathrm{ME}} C_{\mathrm{ACID}} - k_3 C_{\mathrm{NPG}} C_{\mathrm{DE}} + k_{-3} C_{\mathrm{ME}}^2 + r_{\mathrm{W}} M_{\mathrm{W}} C_{\mathrm{DE}} \tag{4.40}$$

The equilibrium constant for the disproportionation reaction is defined as

$$K_3 = \frac{k_3}{k_{-3}} \tag{4.41}$$

Temperature dependence of the reaction rate coefficients is expressed by the Arrhenius law.

$$k_j = k_{j,\mathrm{mean}} \exp\left(-\frac{E_j}{R} \left(\frac{1}{T} - \frac{1}{T_{\mathrm{mean}}} \right) \right) \tag{4.42}$$

where: $k_{j,\mathrm{mean}}$ the apparent reaction rate constant of reaction j at some "mean" temperature value between the minimum and maximum used in the experiments
E activation energy

The kinetic model formed by Equations 4.37 to 4.40 and Equation 4.42 has seven parameters, which are $k_{1,\mathrm{mean}}$, $k_{2,\mathrm{mean}}$, $k_{3,\mathrm{mean}}$, E_1, E_2, E_3 and K_3 (**IV**, p. 6239–6240).

4.4 Skeletal isomerization of 1-pentene

Reactions of 1-pentene were modelled using a pseudohomogeneous model following the reaction mechanism presented in Reactions 28–33. Kinetic parameters were fitted using experimental data determined for the groups of *n*-pentenes, isopentenes, fragmentation and dimerization products.

The weight hourly space velocity has been defined

$$\mathrm{WHSV} = \frac{\dot{m}_\mathrm{F}}{m_\mathrm{C}} \tag{4.43}$$

where: $\dot{m}_\mathrm{F}$ the mass flow rate of a reactant
m_C the mass of the catalyst

Molar flow rate of a reactant can be calculated from

$$\dot{n}_\mathrm{F} = \dot{m}_\mathrm{F} \sum_i \frac{w_i}{M_i} \tag{4.44}$$

where: w_i the mass fraction of component *i* in reactant
M a molar mass.

When adapting Equations 4.43 and 4.44 Equation 4.45 can be written

$$m_\mathrm{C} = \frac{\dot{n}_\mathrm{F}}{\sum_i \frac{w_i}{M_i}} \left(1/\mathrm{WHSV}\right) \tag{4.45}$$

The amount of inert compounds (about 57 wt-%, mostly pentane, **V**, p. 2) was about the same as the amount of C_5 and C_6 compounds in a typical composition of FCC (fluid catalytic cracking) light gasoline (Ignatius *et al.*, 1995). Because the amount of diluent is rather high, the partial pressure of dimerization products is low, and fragmentation products is produced via dimerization products (**V**, Figure 7 and 8) the reaction rates for pentenes (P), isopentenes (I), dimerization (D) and fragmentation (F) products can be calculated from Equations 4.46–4.49, when Equation 4.45 have been differentiated (**V**, p. 4643).

$$r_{\mathrm{P}} = \frac{d\dot{n}_{\mathrm{P}}}{dm_{\mathrm{C}}} = \frac{d\dot{n}_{\mathrm{P}}}{\dot{n}_{\mathrm{F}}} \frac{\sum_i \frac{w_i}{M_i}}{d\left(1/\mathrm{WHSV}\right)} = \frac{dx_{\mathrm{P}}}{d\left(1/\mathrm{WHSV}\right)} \sum_i \frac{w_i}{M_i}$$

$$= -k_{\mathrm{PI}}\left(\frac{p_{\mathrm{P}}}{p^{\theta}}\right) + k_{\mathrm{IP}}\left(\frac{p_{\mathrm{I}}}{p^{\theta}}\right) - k_{\mathrm{PID}}\left(\frac{p_{\mathrm{P}}}{p^{\theta}}\right)\left(\frac{p_{\mathrm{I}}}{p^{\theta}}\right) - 2k_{\mathrm{PD}}\left(\frac{p_{\mathrm{P}}}{p^{\theta}}\right)^2 \tag{4.46}$$

Accordingly

$$r_{\mathrm{I}} = \frac{d\dot{n}_{\mathrm{I}}}{dm_{\mathrm{C}}} = \frac{dx_{\mathrm{I}}}{d(1/\mathrm{WHSV})} \sum_i \frac{w_i}{M_i} = k_{\mathrm{PI}}\left(\frac{p_{\mathrm{P}}}{p^{\theta}}\right) - k_{\mathrm{IP}}\left(\frac{p_{\mathrm{I}}}{p^{\theta}}\right) - k_{\mathrm{PID}}\left(\frac{p_{\mathrm{P}}}{p^{\theta}}\right)\left(\frac{p_{\mathrm{I}}}{p^{\theta}}\right) - 2k_{\mathrm{ID}}\left(\frac{p_{\mathrm{I}}}{p^{\theta}}\right)^2 \tag{4.47}$$

$$r_{\mathrm{D}} = \frac{d\dot{n}_{\mathrm{D}}}{dm_{\mathrm{C}}} = \frac{dx_{\mathrm{D}}}{d(1/\mathrm{WHSV})} \sum_i \frac{w_i}{M_i} = k_{\mathrm{PD}}\left(\frac{p_{\mathrm{P}}}{p^{\theta}}\right)^2 + k_{\mathrm{ID}}\left(\frac{p_{\mathrm{I}}}{p^{\theta}}\right)^2 + k_{\mathrm{PID}}\left(\frac{p_{\mathrm{P}}}{p^{\theta}}\right)\left(\frac{p_{\mathrm{I}}}{p^{\theta}}\right) - k_{\mathrm{DF}}\left(\frac{p_{\mathrm{D}}}{p^{\theta}}\right) \tag{4.48}$$

$$r_{\mathrm{F}} = \frac{d\dot{n}_{\mathrm{F}}}{dm_{\mathrm{C}}} = \frac{dx_{\mathrm{F}}}{d(1/\mathrm{WHSV})} \sum_i \frac{w_i}{M_i} = 2k_{\mathrm{DF}}\left(\frac{p_{\mathrm{D}}}{p^{\theta}}\right) \tag{4.49}$$

where: x_i the molar fraction component i,
p_i the partial pressure of component i,
p^{θ} the pressure of standard state
k an apparent reaction rate constant.

The temperature dependence of the reaction rate coefficients is expressed by the Arrhenius law (Equation 4.42). When adapting monomolecular reaction mechanism (Equations 4.46–4.49 and 4.42) 12 parameters are needed: $k_{\mathrm{PI,mean}}$, $k_{\mathrm{IP,mean}}$, $k_{\mathrm{PD,mean}}$, $k_{\mathrm{ID,mean}}$, $k_{\mathrm{PID,mean}}$, $k_{\mathrm{DF,mean}}$, E_{PI}, E_{IP}, E_{PD}, E_{ID}, E_{PID}, and E_{DF} (**V**, p. 4644).

5 PARAMETER ESTIMATION

5.1 Parameter estimation for BB and MB dehydrocyclization reaction mechanisms

In manuscripts **I** and **II** parameter estimation was performed using a program package that consisted of routines for least squares minimization and integration of ordinary differential equations (Press *et al.*, 1986). Numerical integration of the rate equations was performed by using fifth-order Cash-Karp Runge-Kutta method. Kinetic parameters for the pseudohomogenous model were fitted using the downhill simplex method of Nelder and Mead in order to minimize least squares.

Computer program consisted of main program (Fitter) and subroutines (AMOEBA, Function Evaluation, Todeint, Tderivs, TRKQS, TRKCK). Flow chart of computer program is depicted in Figure 5.1.

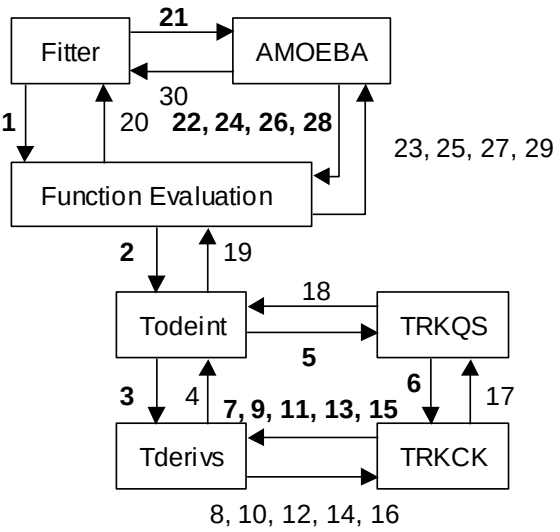

Figure 5.1 Flow chart of fitting computer program. Numbers on arrows mean execution order: bolded numbers subroutine calls, normal numbers end of subroutines.

In main program (Fitter) the amount of parameters, differential equations, data points and the values of data points is fed. In addition the initial simplex is given by means of minimum and maximum value guess for parameters to be fitted. In subroutine Function Evaluation, the sum of least squares is calculated using equation

$$SQ = \sum_{i=1}^{N}\sum_{j=1}^{M}\left(c_{ij}(exp) - c_{ij}(\ fit\ )\right)^2 \qquad (5.1)$$

where c is the amount of component j at the moment i, the symbol *exp* prefers to experimental value and *fit* to fitted value.

Subroutine Todeint is a Runge-Kutta driver with adaptive stepsize control. Differential equations for the reaction mechanism are encoded in the subroutine Tderivs. Subroutine TRKQS is a fifth-order Runge-Kutta step with the monitoring of the local truncation error to ensure accuracy and to adjust stepsize. Subroutine TRKCK uses the fifth-order Cash-Karp Runge-Kutta method to advance the solution over an interval and to return the incremented variables using the given values of variables and their derivatives at a certain point. Subroutine AMOEBA minimizes the multidimensional function using the downhill simplex method of Nelder and Mead **(**Press *et al.*, 1986).

5.2 Parameter estimation for esterification and skeletal isomerization reaction mechanisms

In the manuscripts **III**, **IV** and **V**, the reaction kinetic parameters were first estimated by the usual least squares fitting by minimizing the squared difference between the measured and calculated concentrations (**III** and **IV**) or molar amounts (**V**). The possible cross-correlation and identifiability of parameters were determined using Markov chain Monte Carlo (MCMC) method. Finally using MCMC method, the estimation of model parameters and predictions were performed according to the Bayesian paradigm. A FORTRAN 90 software package MODEST (Haario, 2002) was used for both the least squares and MCMC estimations.

5.2.1 Model parameters in Bayesian terms

The general form of the parameter estimation framework is given as two equations (Solonen, 2008)

$$s = f(x,\theta) \tag{5.2}$$

where: s the model state (e.g. concentration of compounds)
x the design variables (e.g. temperature)
θ the unknown parameters in the model

$$y = g(s) + \varepsilon \tag{5.3}$$

where: y the response that is observed (e.g. a part of the state vector)
g the observation function that maps the model state to the observations
ε the experimental error

In Bayesian statistics, the goal is to find the posterior distribution of parameters θ given measurements y. The posterior distribution is defined using Bayes' rule

$$\pi(\theta|y) = \frac{L(y|\theta)p(\theta)}{\int L(y|\theta)p(\theta)d\theta} \tag{5.4}$$

where: $\pi(\theta|y)$ the posterior distribution of parameters θ given measurements y
L the likelihood, probability of obtaining measurements y if the true parameter value is θ
p the prior, contains all a priori knowledge about the unknown parameter (previous studies, constraints etc.)

The prior signifies the modeller's honest opinion about the unknown. This usually means using very wide priors, or even setting $p(\theta) \equiv 1$ for some or all of the components of the unknown (Laine, 2008). The likelihood here is defined by assuming independent and identically distributed Gaussian errors for the number of observations

$$L(y|\theta) = \prod_{i=1}^{N} L(y_i|\theta) = (2\pi\sigma^2)^{-\frac{N}{2}} exp\left(-\frac{1}{2\sigma^2} SS(\theta)\right) \tag{5.5}$$

where: N the number of observations
σ^2 measurement error variance

$$SS(\theta) = \sum_{i=1}^{N} [y_i - g(f(x_i, \theta))]^2 \quad (5.6)$$

Measurement error variance is estimated using "mean squared error" (MSE) estimate

$$\sigma^2 = \frac{RSS}{N - p} \quad (5.7)$$

where: RSS the sum of least squares in optimum
p the amount of parameters

5.2.2 Markov chain Monte Carlo method

The normalizing constant (the integral in the denominator of the Bayes formula (Equation 5.4)) makes computation of the posterior distribution a difficult problem, especially in multidimensional cases. This problem can be solved only by simulation methods. In MCMC simulation a sequence of values, which follow a stochastic process called a Markov chain, is produced. This sequence of values ($\theta^0, \theta^1, \ldots, \theta^N$) is needed as a sample of the posterior distribution $\pi(\theta|y)$ (Laine, 2008).

These set of samples from the posterior distribution can be used to examine the correlation and accuracy of model parameters and predictions. Thus, MCMC will find many parameter values with which the model fits the data with the accuracy of the measurement error (Solonen, 2008).

5.2.3 The coefficient of determination

The most common measure for the goodness of the fit is the coefficient of determination (Haario, 2002). It is given by the expression

$$R^2 = 100\left(1 - \frac{\|y - y_p\|^2}{\|y - \bar{y}\|^2}\right) \quad (5.7)$$

where: y_p the response that is calculated using model
$\bar{y}$ the average value of all the data points

The closer the value of the coefficient of determination is the number 100, the more perfect is the fit. It should have values well above 90.

6 RESULTS AND DISCUSSION

6.1 Dehydrocyclization of BB

When dehydrocyclizing BB the main reactions were dehydrogenation, hydrogenation, fragmentation, skeletal isomerization and 1,5- and 1,6-cyclization. When the double bond of BeB isomerized, a thermodynamical equilibrium mixture was always resulted (Csicsery, 1968). Moreover, it seemed probable that 1,5-cyclized products (methylindanes and -indenes) reacted further by dealkylation polymerization to form coke (**I**, Scheme 1).

During the first 20 min on-stream, a marked change was observed in the properties of both the fresh and regenerated self-prepared Cr_2O_3/Al_2O_3 -catalyst when using BB or 4-phenyl-1-butene as the reactants (**I**, Figure 1). After 40 min on-stream time the selectivities of products stabilized, and catalysts became deactivate slowly. The total conversion decreased monotonously, which seems to rule out the possibility that the change was due to incomplete reduction of the catalyst. At the initial stages of coking the apparent increase in BB dehydrogenation activity was partly due to elimination of the reverse hydrogenation reaction (**I**, Figure 1b). The disappearance of hydrogenation, skeletal isomerization and fragmentation activities was balanced by isomerization to the other BeB and by cyclization reactions (**I**, Figure 1).

According to the initial-rate experiments 1,5- and 1,6-cyclization reactions proceeded mainly via BeB (**I**, Table 1). 1,6-Cyclization seemed to proceed by a consecutive mechanism via tetralin and dihydronaphthalene to naphthalene (**I**, Scheme 1). At low conversions BB yielded approximately equal amounts of tetralin and dihydronaphthalene, and only at the highest temperature small amounts of naphthalene were observed. Naphthalene became the major product with longer residence times (1/WHSV) (**I**, Figure 6).

The dehydrogenation rate constant obtained in the integral-rate experiments (**I**, Table 1) agreed rather well with that obtained in the initial-rate experiments (**I**, p. 2107), but the hydrogenation reaction seemed to be far more important than suggested by the initial-rate experiments (**I**, p. 2107).

Furthermore, the experiments showed that the 1,6-cyclization rate constant via BeB was much larger in the integral-rate experiments than in the initial-rate experiments. These discrepancies may be due to different reactivities of the olefin isomers, because 4-phenyl-1-butene is thermodynamically unstable, and it isomerizes when using longer residence times. According to these experiments, and one experiment using 4-phenyl-1-butene with longer residence time (**I**, p. 2107) the reactivity for 4-phenyl-1-butene is lower than for other isomers. Obviously, the cyclization rate strongly depends on the structure of those isomers.

6.2 Dehydrocyclization of MB

When dehydrocyclizing MB, it could be noticed or assumed based on BB experiments that the reactions were the following:

Major reactions:
1. Fragmentation of MB
2. Fragmentation of MBes
3. Dehydrogenation of MB
4. Double bond transfer of MBes
5. Hydrogenation of MBes
6. 1,6-Cyclization of MBes

Minor reactions:
7. 1,5-Cyclization of MBes
8. 1,5-Cyclization of MB
9. Methyl group fragmentation of 1,6-cyclization products

There were two reaction types that could not be analyzed: skeletal isomerization of MB and MBes and further reaction of 1,5-cyclization products (**II**, Figure 1).

As to MB dehydrogenation products, it is possible to to produce six MBes isomers although only five of them were detected. The double bond transfer reaction was fast enough, which could be noticed since it reached a chemical equilibrium. In all experiments in spite of the conversion level and the catalyst, the proportional amounts of different MBes isomers were about the same (**II**, Table 1).

Out of ten possible dimethylnaphthalene isomers four isomers were identified. They were 1,5-, 1,6-, 2,6- and 2,7-DMN. Because 2,7-DMN is not the member of the isomerization tendency group (1,5-, 1,6- and 2,6-DMN) (Takagawa *et al.*, 1994), it is plausible to assume that one impurity of reactant, i.e. 1-(*p*-tolyl)-3-methylbutane, dehydrogenated and cyclized into 2,7-DMN (Shimada *et al.*, 1993). The amount of 2,7-DMN was about 2 wt-%, and the amounts of 1,5- and 1,6-DMN were negligible.

Product selectivity changed radically during precoking period (one hour) when Cr_2O_3/Al_2O_3 or 4.7 wt-% potassium impregnated Cr_2O_3/Al_2O_3 was used as a catalyst, but it remained rather stable after one hour on-stream time (**II**, Figures 3 and 4). At the beginning of the precoking period fragmentation activity was high, and against expectations, it even increased when potassium impregnated Cr_2O_3/Al_2O_3 was used, because fragmentation is an acid catalyzed reaction. Potassium impregnation also diminished the Brunauer-Emmett-Teller (BET) surface, and according to the experiments fragmentation occurred without catalyst. Probably, these two facts explain the increased fragmentation activity compared to other reactions while using potassium impregnated Cr_2O_3/Al_2O_3 (**II**, p. 4024).

During precoking period at high conversion level it was possible to get almost 100 mol-% selectivities of fragmentation products while using potassium impregnated Cr_2O_3/Al_2O_3. Some acidity was also left, after potassium impregnation, because the catalyst adsorbed 22 μmol/g ammonia (Laatikainen *et al*., 1996). Hence, one possible explanation for increased fragmentation is that the ratio of weak/strong acidic sites of Al_2O_3 increased substantially as a consequence of potassium impregnation. Strong acidic sites can be regarded as the Lewis sites, because alkali promoters eliminate Lewis acidity by forming superficial chromate which is not acidic (Damon and Scokart, 1980). Those weak acidic sites (Brönsted sites) caused the major part of fragmentation, and they deactivated at the beginning of precoking period. Not until after that other reactions were possible (**II**, p. 4024).

During fast deactivation period 1,6/1,5 –cyclization ratio changed radically when using Cr_2O_3/Al_2O_3 or potassium impregnated Cr_2O_3/Al_2O_3 -catalyst at high conversion level. At the

conversion level almost 100 mol-% 1,6/1,5 –cyclization ratio was over 40, but it decreased into 10 at the conversion level under 80 mol-% when unimpregnated Cr_2O_3/Al_2O_3 –catalyst was used. When Pt/SiO_2 and $V/Ca/Al_2O_3$ –catalysts were used, the ratio was below 5 at the conversion level of 40-90 mol-% (**II**, Figure 5).

According to the modeling results, potassium impregnation did not affect to the apparent reaction rate constant of 1,6-cyclization products, or it even promoted 1,6-cyclization slightly (**II**, Table 2). Instead of, the apparent reaction rate constant of 1,5-cyclization products decreased by a factor almost 0.5, due to the decrease of acidity as a consequence of potassium impregnation (Csicsery, 1967) (II, p. 4024).

Concerning fragmentation Cr_2O_3/Al_2O_3 and $V/Ca/Al_2O_3$ –catalyst functioned similarly during precoking period, because of the acidic Al_2O_3 support. Because Pt/SiO_2 had neutral SiO_2 support, the fragmentation activity was lower, and product selectivities remained rather constant during experiments although the conversion was high. The 1,6/1,5-cyclization ratio remained about the same regardless for $V/Ca/Al_2O_3$ or Pt/SiO_2 –catalyst, but it increased slightly for Cr_2O_3/Al_2O_3 (**II**, Figure 5). In addition, Pt/SiO_2 –catalyst seemed to dealkylate 1,6-cyclization products more efficiently than Cr_2O_3/Al_2O_3 (**II**, Table 2) (**II**, p. 4024).

6.3 Esterification of NPG with different carboxylic acids

When performing esterification of NPG with PRO, IBA or EHA, NPG was esterified to ME and water followed by ME esterification to DE and water. In disproportionation, 2 ME molecules formed NPG and DE (**III**, Figure 7). Water was removed from the reactor in order to prevent the reverse reaction.

In esterification of NPG with PRO, IBA or EHA, the formation of the corresponding monoester was clearly much faster than the consecutive esterification of the monoester to diester (**IV**, Figure 4). For IBA the ratio of the apparent reaction rate constants for the corresponding reactions (k_1/k_2) was about 5.2 at 383 K when using Dowex (0.27 wt-%) as a catalyst (**IV**, Figure 5c). For PRO with

smaller molecule size, the ratio was 2.8, and for EHA with larger molecule size, the ratio was 9.3. These ratios are quite unreliable, since the further esterification of monoester to diester (k_2) is a secondary and minor reaction. Nevertheless, it gives a clue to the fact that it is much more difficult to produce diesters from monoesters of large molecules than of small ones. Of course, when the size of the acid molecule is increased the apparent reaction rate constant of NPG esterification to monoester (k_1) decreases (**IV**, Figure 5a). For PRO the apparent reaction rate constant was 4.35×10^{-3} kg mol^{-1} min^{-1} and for IBA and EHA it was 2.01×10^{-3} and 0.19×10^{-3} kg mol^{-1} min^{-1} over Dowex (0.27 wt-%) at 383 K, respectively (**IV**, p. 6241).

The rate of esterification has been found by several authors to decrease with increasing crosslinking in the resin particles (Bhagade and Nageshwar, 1978; Gomzi and Pajc, 1970). This agrees well with the current results as the esterification activity was clearly higher when using a gellular type resin (Dowex 50WX2) than when using a macroreticular type resin (Amberlyst 15) (**IV**, Figure 6). Crosslinkage-%DVB of Amberlyst 15 was as high as 20–25 whereas crosslinkage-%DVB of Dowex 50WX2 was only two. The ratio of the apparent reaction rate constants for the resins (k_1(Dowex)/k_1(Amb)) was over two when performing esterification of NPG with IBA, although their ion-exchange capacities are about the same (**IV**, Table 2). The most active catalyst was naturally *para*-toluene sulfonic acid because of its homogeneous nature (**IV**, p. 6245).

The esterification reactions proceeded also without a catalyst (**IV**, Figure 5 and Table 3). The self-catalyzed reaction rate evidently contributes to esterification at low catalyst loadings when comparing the self-catalyzed reaction rate with that of the ion-exchange resin catalyzed (Kolah *et al.*. 2007). Catalyzed (Dowex 50WX2) and self-catalyzed esterification reaction rate constants of PA and IBA differed clearly, but those of EHA do not necessarily differ so much because of its larger size (**IV**, p. 6246).

Only slight differencies concerning monoester selectivities between catalysts were obtained when the conversion of NPG was over 50 mol-%. According to these results the selectivity decreased in the order of Amberlyst 15 > Dowex 50 WX 2 > *para*-toluene sulfonic acid (Figure 6.1). In literature, when the gellular type resin is changed to macroreticular one, the selectivity increase

more than in these experiments (Chakrabarti and Sharma, 1993; Helfferich, 1962; Pitochelli, 1980). Increasing carbon atoms of acid molecule (EHA>IBA>PRO) increased the monoester selectivity.

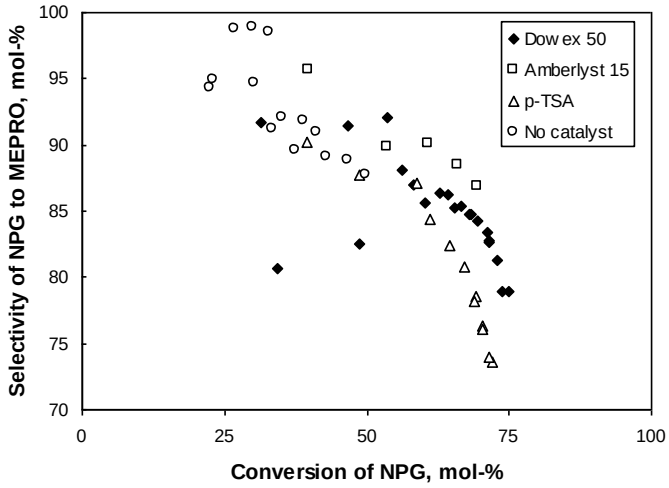

Figure 6.1 The selectivity of NPG to MEPRO (NPG/PRO 1/1 mol/mol) at reaction temperatures between 373–408 K.

One equilibrium reaction that was also discovered was the disproportionation reaction. The esterification experiments can be explained without disproportionation, but experimentally it certainly takes place (**III**). It was a minor reaction in the mechanism but its existence could, however, be experimentally verified using NPG and DEPRO (**III**, Figure 5) , MEPRO (**III**, Figure 4) and MEIBA (**IV**, Figure 7) as reactants. The equilibrium constant of disproportionation varied between 3 and 6 (**IV**, Table 3).

6.4 Skeletal isomerization of 1-pentene

When isomerizing 1-pentene three different kinds of isomerization reactions were detected: double bond, *cis-trans* and skeletal isomerization (**V**, Figure 7). Minor side reactions were dimerization and fragmentation.

HZSM-22 –catalyst was very active and selective concerning the production of isopentenes. In most experiments, it deactivated slowly. When the conversion level was just below the equilibrium conversion of the skeletal isomerization reaction (*n*-pentenes ⇄ isopentenes, about 80 mol-%) the selectivity to isopentenes was over 95 mol-% (**V**, Fig. 5). At conversion levels above this point, the selectivity to isopentenes decreased drastically. Considering side reactions, the selectivity to dimerization and fragmentation decreased as a function of the time on-stream, while that of skeletal isomerization increased (**V**, Figure 1). Probably, at the beginning, the strongest acid sites deactivated, which caused the decrease of the selectivity to minor products. The acid strength required for acid-catalyzed conversions of hydrocarbons may be ranked as: cracking ~ oligomerization > skeletal isomerization >> double-bond isomerization (O'Young *et al.*, 1994).

It was assumed that three separate reactions produced dimerization products, namely dimerization between

1. two *n*-pentene molecules
2. two isopentene molecules
3. *n*-pentene and isopentene molecules

According to the modeling results obtained in this study, the second dimerization reaction is negligible and most of the dimerization products come from the reaction between *n*-pentene molecules, and between *n*-pentene and isopentene molecules (**V**, Figure 14). When the Arrhenius parameters of these dimerization reactions were allowed to identify freely, the range of uncertainty of these parameters was large and standard errors were very high (**V**, Figure 10 and Table 2). As a consequence of these results uncertainty estimates of the apparent reaction rate constants (**V**, Figure 14) were also large. Particularly, the values of the apparent reaction rate constants of the dimerization reactions between isopentene molecules, and between *n*-pentene and isopentene molecules, could vary in a large scale. For this reason it was necessary to assume that the apparent reaction rate constants of dimerization reactions are equal ($k_{PD} = k_{ID} = k_{PID}$). A consequence of this assumption was that the Arrhenius parameters of the dimerization reactions were identified quite well (**V**, Figures. 12, 15 and Table 2) (**V**, p. 4648).

At the rather low temperatures used, between 523−598 K, monomolecular fragmentation can be ignored. The slow rate of monomolecular cracking allows dimerization-cracking and various side reactions to become significant with a pentene feed (Buchanan et al., 1996). Furthermore, cracking rates increase dramatically with the carbon number of an olefin, because more energetically favorable modes become available for β-scission of the carbenium ion formed by proton donation (Buchanan et al., 1996). Even though some monomolecular fragmentation of 1-pentene may have occurred, it could not be detected (**V**, p. 4648).

Monomolecular (Houžvicka et al., 1996; Houžvicka and Ponec, 1997) and bimolecular (Guisnet et al., 1996; Guisnet et al., 1998) reaction mechanisms have been proposed for skeletal isomerization of 1-butene to isobutenes. When using a ferrierite catalyst it has been observed that a bimolecular process operates on the non-selective catalyst, while a monomolecular process exists on the selective catalyst (Meriaudeau et al., 1996). Both monomolecular (**V** Figure 7) and bimolecular (dimerization-fragmentation) (**V**, Figure 8) reaction mechanisms were considered, when performing skeletal isomerization of 1-pentene to isopentenes. Based on the fitting results, both reaction mechanisms explained skeletal isomerization of 1-pentene to isopentenes (**V**, Table 2). However, the monomolecular reaction mechanism explained the formation of dimerization and fragmentation products slightly better (**V**, Figure 13) (**V**, p. 4647).

7 CONCLUSIONS

7.1 Dehydrocyclization of BB

The changes of the product composition during coking and the kinetic data indicated that cyclization of BB proceeds predominantly via the olefinic (BeB) intermediates. The discrepancy between the initial-rate and integral-rate data also suggested that the cyclization rate strongly depends on the structure of these olefinic intermediates. 1-Phenyl-1-butenes were shown to be the primary products of the dehydrogenation step. No expansion of the five-membered ring to a six-membered ring took place according to the experiments with the methylindene mixture as a feed. The 1,5-cyclization products seemed not to be stable at the condition studied. They were assumed to dealkylate and polymerize.

7.2 Dehydrocyclization of MB

Based on the BB experiments with coked catalyst MB was assumed to cyclize via the olefinic (MBes) intermediates. The 1,5-cyclization products were assumed to dealkylate and polymerize and not to expand six-membered ring. Concerning DMNs, all of the tested catalysts produced 2,6-DMN selectively. Out of ten possible DMN isomers, 1,5-, 1,6-, 2,6- and 2,7-DMN were identified. The amount of 2,7-DMN was about 2 wt-%, and the amounts of 1,5- and 1,6-DMN were negligible. According to the modeling results, potassium impregnation of chromia/alumina -catalyst did not affect the reaction rate constant of 1,6-cyclization products, or it even promoted 1,6-cyclization slightly. Naturally, the amount of the acid catalyzed reaction (1,5-cyclization) products decreased as a consequence of potassium impregnation. Potassium impregnation also decreased the activity of chromia/alumina. $V/Ca/Al_2O_3$ (5 wt-% vanadium) and Pt/SiO_2 (1 wt-% platinum) were slightly more active than unimpregnated chromia/alumina.

7.3 Esterification of NPG with different carboxylic acids

In esterification of NPG with PRO, IBA or EHA the formation of the corresponding monoester was clearly much faster than the consecutive esterification of the monoester to diester. One experimentally verified side reaction was the disproportionation of ME. The esterification activity was clearly higher when using a gellular type resin (Dowex 50WX2) than when using a macroreticular type resin (Amberlyst 15). The most active catalyst was *para*-toluene sulfonic acid because of its homogeneous nature. The esterification reactions proceeded also without a catalyst. Increasing carbon atoms of acid molecule (EHA>IBA>PRO) increased the monoester selectivity. The selectivity order of the catalyst was: Amberlyst 15 > Dowex 50 WX 2 > *para*-toluene sulfonic acid.

7.4 Skeletal isomerization of 1-pentene

When isomerizing 1-pentene three different kinds of isomerization reactions were detected: double bond, *cis-trans* and skeletal isomerization. Minor side reactions were dimerization and fragmentation. HZSM-22 –catalyst was very active and selective concerning the production of isopentenes. When the conversion level was just below the equilibrium conversion of the skeletal isomerization reaction (about 80 mol-%) the selectivity to isopentenes was over 95 mol-%. Based on the fitting results, both mono- and bimolecular reaction mechanisms explained skeletal isomerization of 1-pentene to isopentenes.

REFERENCES

Abbot, J., Wojciechowski, B.W., The Mechanism of Catalytic Cracking of *n*-Alkenes on ZSM-5 zeolite. *Can. J. Chem. Eng. 63*, 462–469 (1985).

Abbot, J., Wojciechowski, B.W., Kinetics and Selectivity of Reactions of 1-Alkenes on HY Zeolite: the Influence in Chain Length. *Can. J. Chem. Eng. 66*, 817–824 (1988).

Abe, T., Ebata, S., Machida, H., Kida, K., Process for Production of 2,6-Dimethylnaphthalene. Eur. Pat. Appl. EP 362,651 (1990).

Abe, T., Uchiyama, S., Ojima, T., Kida, K., Process for Production of 2,6-Dimethylnaphthalene. Eur. Pat. Appl. EP 362,507 (1990).

Arnaudov, S., Dimitrov, C., Catalytic Conversion of 1-Phenyl-butene-3, 1-Phenylbutene-2 and 1-Phenylbutene-1 on Silica-Alumina Catalyst (in Bulgarian). *Annu. Univ. Sofia, Fac. Chim. 64*, 343–352 (1969/1970).

Astle, M. J., Schaeffer, B., Obenland, C. O., Esterification of Glycols by Acids in the Presence of Cation Exchange Resins. *J. Am. Chem. Soc. 77*, 3643–3644 (1955).

Bäck, S.H., Lee, W.Y., Skeletal Isomerization of 1-Butene to Isobutene over Mg-ZSM-22. *Appl. Catal. 164*, 291–301 (1997).

Bhagade, S. S., Nageshwar, G. D. Catalysis by Ion Echange Resins-Esterification. *Chem. Petrochem. J. 9*, 3–12 (1978).

Buchanan, J.S., Santiesteban, J. G., Haag, W.O., Mechanistic Considerations in Acid-Catalyzed Cracking of Olefins. J. *Cat.* 158, 279–287(1996).

Byggningsbacka, R., Lindfors, L.-E., Kumar, N., Catalytic Activity of ZSM-22 Zeolites in the Skeletal Isomerization Reaction of 1-Butene. *Ind. Eng. Chem. Res. 36*, 2990–2995 (1997).

Byggningsbacka, R., Kumar, N., Lindfors, L.-E., Comparative Study of the Catalytic Properties of ZSM-22 and ZSM-35/Ferrierite Zeolites in the Skeletal Isomerization of 1-Butene. *J. Catal. 178*, 611–620 (1998).

Chakrabarti, A., Sharma, M. M., Cationic Ion Exchange Resins as Catalyst. *React. Polym. 20*, 1–45 (1993).

Chase, J.D., Woods, J.H., MTBE and TAME – a Good Octane Boosting Combo. *Oil & Gas Journal 15*, 149–152 (1979).

Cheng, Z.X., Ponec, V., Selective Isomerization of Butene to Isobutene. *J. Catal. 148*, 607–616 (1994).

Csicsery, S., Reactions of *n*-Butylbenzene over Supported Platinum Catalysts. *J. Catal. 9,* 336–357 (1967).

Csicsery, S., The Reactions of *n*-Butylbenzene over Nonacidic Chromia-Alumina. *J. Catal. 9,* 416–420 (1968).

Damon, J. P., Scokart, P. O., Acid-Base Properties of Alkali Promoted Chromia-Alumina Catalysts. *Chem. Lett.*, 327 (1980).

Duplan, J.-L., Amigues, P., Verstraete, J., Travers, Ch., Kinetic Studies of the Skeletal Isomerization of *n*-Pentenes over the ISO-5 Process Catalyst. *Proc.-Ethylene Prod. Conf. 5*, 429–449 (1996).

Fité, C., Iborra, M., Tejero, J., Izquierdo, J. F., Cunill, F., Kinetics of the Liquid-Phase Synthesis of Ethyl *tert*-Butyl Ether (ETBE). *Ind. Eng. Chem. Res. 33*, 581–591 (1994).

Friel, J. M., Coating Compositions Containing Mono- or Diester Coalescing Agents and a Substrate Coated Therewith. Eur. Pat. Appl. EP0026982 (1981).

Gates, B.C., Kazer, J.R., Schuit, G.C.A., *Chemistry of Catalytic Processes*; McGraw-Hill: New York, 1979.

Gomzi, Z., Pajc, E., Esterification of 1-Butanol with Acetic Acid with an Ion Exchange Resin as Catalyst. *Kem. Ind. 19*, 294 (1970).

Guisnet, M., Andy, P, Gnep, N.S., Benazzi, E., Travers, C., Skeletal Isomerization of *n*-Butenes I. Mechanism of *n*-Butene Transformation on a Nondeactivated H-Ferrierite Catalyst. *J. Catal. 158*, 551–560 (1996).

Guisnet, M., Andy, P, Gnep, N.S., Travers, C., Benazzi, E. Comments on "Skeletal Isomerization of Butene: On the Role of the Bimolecular Mechanism". *Ind. Eng. Chem. Res. 37*, 300–302 (1998).

Haario, H., *Modest. User's Guide*, ProfMath Oy, Helsinki, Finland, 2002.

Helfferich, F. *Ion Exchange*, McGraw-Hill, New York, 1962.

Houžvicka, J., Diefenbach, O., Ponec, V., The Role of Bimolecular Mechanism in the Skeletal Isomerisation of *n*-Butene to Isobutene. *J. Catal. 164*, 288–300 (1996).

Houžvicka, J., Ponec, V., Skeletal Isomerization of Butene: On the Role of the Bimolecular Mechanism. *Ind. Eng. Chem. Res. 36*, 1424–1430 (1997).

Houžvicka, J., Hansildaar, S., Ponec, V., The Shape Selectivity in the Skeletal Isomerisation of *n*-Butene to Isobutene. *J. Catal. 167*, 273–278 (1997).

Huijts, R. A., de Vries, A. J., Mechanical Behavior of Poly(Ethylene 2,6-Naphthalene-Dicarboxylate) (PEN) Fibres Near the Glass-Rubber Transition Temperature. *Intern. J. Polymer Mater. 22*, 231–236 (1993).

Ignatius J., Järvelin, H., Lindqvist, P., Use TAME and Heavier Ethers to Improve Gasoline Properties. *Hydrocarbon Processing 74*(2), 51–53 (1995).

Inamasi, K.; Fushimi, N.; Takagawe, M. Process for Production of 2,6-Dimethylnaphthalene. Eur. Pat. Appl. EP 546,266 (1993).

Kiricsi, I, Koskimies, S., Csicsery, S., Preparation of 1-(2-Methylbutyl)-4-methylbenzene. PCT Int. Appl. WO 9724305 (1997).

Kolah, A.K., Asthana, N.S., Vu, D.T, Lira, C.T., Miller, D.J., Reaction Kinetics of the Catalytic Esterification of Citric Acid with Ethanol. *Ind. Eng. Chem. Res. 46*, 3180(2007).

Laatikainen, M., Sahala K.-M., Vahteristo, K., Lindström, M., *Effect of Potassium Promoter on Dehydrocyclization of n-Butylbenzene over Chromia-Alumina*, Lappeenranta University of Technology, Publication 66, Lappeenranta, Finland, 1996.

Laine, M., *Adaptive MCMC Methods with Applications in Environmental and Geophysical Model*., Ph.D. Dissertation, Finnish Meteorological Institute, Helsinki, Finland, 2008.

Mazzotti, M., Kruglov, A., Neri, B., Gelosa, D., Morbidelli, M., A Continuous Chromatographic Reactor: SMBR. *Ind. Eng. Chem. Res. 51*, 1827–1836 (1996).

Mazzotti, M., Neri, B., Gelosa, D., Kruglov, A., Morbidelli, M., Kinetics of Liquid-Phase Esterification Catalyzed by Acidic Resins. *Ind. Eng. Chem. Res. 36*, 3–10 (1997).

Meeks, E., Coupling Computational Fluid Dynamics with Chemistry and Physics. *CHEMICAL INNOVATION 1*, 21 (2000).

Meier, W.M., Olson, D.H., *Atlas of Zeolite Structure Types*, 2nd ed.; Butterworth-Heinemann: USA, 1987.

Mitsui Petrochemical Industries LTD. Process for Preparing Dimethylnaphthalenes. GB 1448136 (1973).

Miyamoto, S., Taniguchi, K., Teranishi, K., Naphthalenes (in Japanese) Jpn. Kokai Tokkyo Koho JP 48,048,458 (1973).

Meriaudeau, P., Bacaud, R., Hung, L.N., Vu, A.T., Isomerisation of Butene in Isobutene on Ferrierite Catalyst: A Mono- or a Bimolecular Process ? *J. Mol. Catal. A: Chemical 110*, L177–L179 (1996).

Mooiweer, H.H., de Jong, K.P., Kraushaar-Czarnetzki, B., Stork, W.H.J., Krutzen, B.C.H., Skeletal Isomerization of Olefins with the Zeolite Ferrierite as Catalyst. *Stud. Surf. Sci. Catal. 84*, 2327-2334 (1994).

Nakamura, S., *Japanese R&D Trend Analysis, Advanced Materials, Phase IV,* Report No. 4, 88−104 (1992).

O'Young, C.-L., Xu, W.-Q., Simon, M., Suib, S.L., Skeletal Isomerization of *n*-Butenes on Zeolite Catalysts: Effects of Acidity. *Stud. Surf. Sci. Catal. 84*, 1671−1676 (1994).

Parra, D., Izquierdo, J. F., Cunill, F., Tejero, J., Fité, C., Iborra, M., Vila, M., Catalytic Activity and Deactivation of Acidic Ion-Exchange Resins in Methyl *tert*-Butyl Ether Liquid-Phase Synthesis. *Ind. Eng. Chem. Res. 37*, 3575-3581 (1998).

Pines, H., Goetschel, C., Alumina: Catalyst and Support XXX. Dehydrogenation and Skeletal Isomerization of Butylbenzenes over Chromia-Alumina Catalysts. *J. Catal. 6*, 371−379 (1966).

Pitochelli, A. R. *Ion Exchange Catalysis and Matrix Effects*; Rohm and Haas: Philadelphia, 1980.

Poole, C. P., Mac Iver, D. S., The Physical-Chemical Properties of Chromia-Alumina Catalysts. *Advances in Catalysis 17*, 223−314 (1967).

Press, W. H., Flannery, B. P., Teukolsky, S. A., Vetterling, V. T., *Numerical Recipes; The Art of Scientific Computing*; Cambridge University Press: Cambridge, U.K., 1986.

Rehfinger, A., Hoffman, U., Kinetics of Methyl Tertiary Butyl Ether Liquid Phase Synthesis Catalyzed by Ion Exchange resin – I. Intrinsic Rate Expression in Liquid Phase Activities. *Chem. Eng. Sci. 45*, 1605−1617 (1990).

Rönnback, R., Salmi, T, Vuori, A., Haario, H., Lehtonen, J., Sundqvist, A., Tirronen, E., Development of a Kinetic Model for the Esterification of Acetic Acid with Methanol in the Presence of a Homogeneous Acid Catalyst. *Chem. Eng. Sci. 52*, 3369−3381 (1997).

Saha, B., Sharma, M. M., Esterification of Formic Acid, Acrylic Acid and Methacrylic Acid with Cyclohexene in Batch and Distillation Column Reactors: Ion-Exchange Resins as Catalysts. *React. Funct. Polym. 28*, 263−278 (1996).

Saukkonen, S., *Butyylibentseenin dehydrosyklisointireaktion kinetiikka*, Diplomityö, Lappeenranta, Finland, 1995.

Shimada, K., Preparing of Alkenylbenzenes (in Japanese) Jpn. Kokai Tokkyo Koho JP 52,137,91 (1993).

Simon, M.W., Suib, S.L., O'Young, C.-L., Synthesis and Characterization of ZSM-22 Zeolites and Their Catalytic Behaviour in 1-Butene Isomerization Reactions, *J. Catal. 147*, 484−493 (1994).

Solonen, A., *Modest MCMC Tutorial Version 0.3*, Laboratory of Applied Mathematics, Lappeenranta University of Technology, 2008.

Takagawa, M., Shigematsu, R., Nagagata, K., Method for Isomerizing Dimethylnaphthalene. Eur. Pat. Appl. EP 618,180 (1994).

Taniguchi, M., Matsuoka, H., 2-Methyl-1-tolylbutane (in Japanese). Jpn. Kokai Tokkyo Koho JP 50,093,925 (1975).

Vahteristo, K., Laatikainen, M., Saukkonen, S., Lindström, M., *Reactions of n-Butylbenzene over Dehydrocyclization Catalysts*, Lappeenranta University of Technology, Publication 72, Lappeenranta, Finland, 1996.

Zhang, A., Nakamura, I., Aimoto, K., Fujimoto, K., Isomerization of *n*-Pentane and Other Light Hydrocarbons on Hybrid Catalyst. Effect of Hydrogen Spillover. *Ind. Eng. Chem. Res. 34*, 1074–1080 (1995).

PART II: THE PUBLICATIONS